

The large D limit of General Relativity

Roberto Emparan^{a,b}, Ryotaku Suzuki^c, Kentaro Tanabe^b

^a*Institució Catalana de Recerca i Estudis Avançats (ICREA)
Passeig Lluís Companys 23, E-08010 Barcelona, Spain*

^b*Departament de Física Fonamental, Institut de Ciències del Cosmos,
Universitat de Barcelona, Martí i Franquès 1, E-08028 Barcelona, Spain*

^c*Department of Physics, Kyoto University, Kyoto 606-8502, Japan*

emparan@ub.edu, ryotaku@tap.scphys.kyoto-u.ac.jp, ktanabe@ffn.ub.es

Abstract

General Relativity simplifies dramatically in the limit that the number of spacetime dimensions D is infinite: it reduces to a theory of non-interacting particles, of finite radius but vanishingly small cross sections, which do not emit nor absorb radiation of any finite frequency. In many respects, black holes and black branes behave like configurations of dust. The simplicity of this limit motivates the study of the theory in an expansion in $1/D$. Large D introduces a separation of scales that allows an effective theory of black hole dynamics. We develop to leading order in $1/D$ this effective description for massless scalar fields and compute analytically the scalar absorption probability. We solve to next-to-next-to-leading order the black brane instability, with very accurate results that improve on previous approximations with other methods. These examples demonstrate that problems that can be formulated in an arbitrary number of dimensions may be tractable in analytic form, and very efficiently so, in the large D expansion.

Contents

1	Introduction	2
2	Large D limit of black holes	4
2.1	‘Smallness’ of the horizon and a hierarchy of scales	5
2.2	Absence of interactions	6
2.3	Other black holes: rotation and other topologies	8
2.4	Charge	11
2.5	Large D in Anti-deSitter	11
3	Sphere of influence	13
3.1	Quasinormal modes	14
3.2	Across the horizon, a small interior	15
4	Classical radiation from black hole interactions	15
4.1	Black hole collisions	15
4.2	Orbiting black holes	17
5	Quantum effects	18
6	Large D effective theory: scalar wave absorption	19
6.1	Near and far regions	19
6.2	Massless scalar wave equation	20
6.3	Integrating out the near region	22
6.4	Far region waves	24
6.5	Matching and analysis of results	25
6.6	Effective scalar wave dynamics	27
6.7	Final remarks	27
7	Black brane instability	29
7.1	Perturbation equations	30
7.2	Far region	31
7.3	Near region	32
7.4	Comparisons and accuracy	35
7.5	Final remarks	36
8	Conclusion	38
	Appendices	40

1 Introduction

The fascination power of General Relativity stems largely from the wealth of physical phenomena that are encoded in equations as simple as

$$R_{\mu\nu} = 0. \tag{1.1}$$

Naturally, this conceptual simplicity unfolds its rich dynamics at the cost of technical complexity. It is very difficult to find closed exact solutions to these coupled, non linear, partial differential equations, for almost any phenomenon of interest unless a substantial degree of symmetry is present.

Physical theories often contain parameters that can be varied in such a way that the theories remain well defined. A fruitful strategy is to focus on regions of the parameter space, usually close to its origin or boundaries, where the theories simplify. Einstein's theory in vacuum, (1.1), appears to have only one natural parameter: the number D of spacetime dimensions. We will argue that in the limit $D \rightarrow \infty$, General Relativity simplifies dramatically, its dynamics becoming trivial at all non-zero length scales. This is a strong motivation for the study of the theory in an expansion in $1/D$.

While it seems unlikely that our universe be infinite-dimensional, the study of General Relativity around this limit can be useful, both to gain a better understanding of the theory and as an approximation scheme for calculations in less unrealistic cases, say $D = 4$ or $D = 10, 11$. We have learned in recent years that new features appear in the spectrum of black hole solutions as D grows beyond four [1]. Still, it may not be unreasonable to expect that some properties remain more robust as D is increased — to begin with, the theory (1.1) does not have black holes nor a dynamical graviton when $D \leq 3$, and always has them for any $D \geq 4$. The question of to what extent an expansion in $1/D$ is a good qualitative guide to moderate D , and if so, how accurate it is, probably depends on the specific problem under consideration. In this article this concern will remain mostly in the background, and instead we will focus on understanding the main properties of the limit and on how to organize calculations in the $1/D$ expansion. Nevertheless, one of our examples shows that these techniques can give very accurate results even at relatively low values of D .

Early studies of gravity in the large D limit analyzed the quantum theory and the properties of its Feynman diagrams [2, 3]. The main motivation is the possible analogy with the large N limit of $SU(N)$ gauge theories — indeed, the local Lorentz group $SO(D-1, 1)$ is the gauge group of gravity. The large N limit of Yang-Mills theories is useful because, although the number of gluons grows unbounded, they arrange themselves into worldsheets of strings (propagating in more dimensions). One might hope that a similar miracle could occur also for large D gravity. However, D appears not only in the number of graviton polarizations but also, more troublingly, in phase space integrals. Actually, taking D to be large seems a bad idea for a quantum field theory, since the ultraviolet behavior

generically worsens. This can be alleviated by focusing on Kaluza-Klein truncations of the spectrum [4, 5], which retain the growing number of polarizations but make the short-distance behavior essentially four-dimensional, with the usual divergence problems in the gravitational sector. We shall not pursue any of these approaches.

Instead, we study mostly the classical theory of eq. (1.1), which is well defined in any D . After all, many quantum properties of gravity are dominated by classical effects such as black hole formation. One speculation is that the illnesses of quantum gravity may be absent outside the horizons when $D \rightarrow \infty$ and might remain under some control close to the horizon in the $1/D$ expansion. At any rate we will see that, even if its quantum version happens to be badly behaved, the large D limit of the classical theory is a useful one.

The study of classical gravity in arbitrary $D \geq 4$ has gained momentum over the years, and it has often seemed natural to examine specific results in the limit $D \rightarrow \infty$. However, very rarely has the large D expansion been pursued as a subject in its own right. A notable exception are refs. [6, 7], which are closest in spirit and techniques to our approach. Nevertheless, their context was restricted to a particular phenomenon (the Euclidean zero mode of the Schwarzschild solutions) and a bigger framework was not developed. Some general observations about black holes and black branes at large D are made in [8, 9] emphasizing slightly different features than here. Although there are many studies of gravitational phenomena in arbitrary D , those that make explicit reference to the large D limit are, as far as we are aware, relatively few, *e.g.*, [10]–[21].

In summary: a systematic approach to the large D limit of classical General Relativity has been lacking so far. We aim to provide some basic entries to the concepts and techniques of this subject.

A main element of our approach is that, in contrast to the studies inspired by large N gauge theories, we will not focus on perturbations around a Minkowski background but rather on non-perturbative objects in the theory, namely its black holes. We argue that in the limit $D \rightarrow \infty$ black holes are in many respects non-interacting particles. They do not attract each other and, even if their radius remains finite, their collision cross sections vanish. They reflect perfectly all radiation of any finite frequency. Some of these features suggest to think of black holes as ‘dust particles’. Black branes do behave like if made of dust, with no tension to hold them together.

The simplicity of this limit makes it a good starting point for a perturbative expansion in $1/D$. We will see that in the limit $D \rightarrow \infty$ the gravitational field vanishes outside the horizon at $r = r_0$, while at large but finite D this field is strongly localized close to the horizon in the region

$$r - r_0 \lesssim \frac{r_0}{D}. \quad (1.2)$$

Crucially, a new scale appears owing to the very steep gradient, $\sim D/r_0$, of the gravitational potential near the horizon. This separation between scales $r_0/D \ll r_0$ allows to develop an effective theory of black hole dynamics. Fields outside the black hole propagate

in an effectively flat spacetime, subject to certain boundary conditions very near the horizons, which replace the black holes. Technically, this is a problem of matched asymptotic expansions. Conceptually, it is an effective theory in which the degrees of freedom for the black hole are integrated out and replaced by boundary conditions on large-distance fields. What is peculiar to this effective theory is that the notion of short-distance degrees of freedom is the result of having large D , instead of the more conventional idea of considering wavelengths much larger than the horizon radius. This results in a much larger range of applicability of the effective theory.

We begin in the next section motivating the ‘small, non-interacting particle’ picture of the limit $D \rightarrow \infty$ through an extensive study of known black hole solutions. In section 3 we introduce the notion of the ‘sphere of influence’ of the black hole. In section 4 we discuss how and when classical gravitational radiation can be emitted through black hole interactions at $D \rightarrow \infty$. In section 5 we make some comments about quantum effects and Hawking radiation in black holes at large D . In section 6 we introduce the $1/D$ expansion in the study of the propagation of massless scalars in the black hole background. We solve the theory in the region near the horizon and find the effective boundary conditions for outside fields. We obtain a compact analytic expression for the scalar absorption probability that is valid over a very wide range of frequencies. In section 7 we solve the spectrum of unstable perturbations of black branes in closed analytic form to next-to-next-to-leading order at large D . The results are very accurate for all but the two lowest dimensions. We conclude in section 8.

2 Large D limit of black holes

We take the point of view that General Relativity in vacuum, the theory of (1.1), is essentially a theory of black holes that interact via the gravitational field between them, and which can emit and absorb gravitational waves through these interactions. We can also include as objects of study the singular plane wave solutions that appear in the infinite boost limit of black holes, but in general we exclude other nakedly singular solutions.

We begin with the most basic solution, the Schwarzschild-Tangherlini spacetime

$$ds^2 = -f dt^2 + f^{-1} dr^2 + r^2 d\Omega_{D-2}, \quad (2.1)$$

$$f(r) = 1 - \left(\frac{r_0}{r}\right)^{D-3}, \quad (2.2)$$

with a horizon of radius r_0 [22]. When we take the limit $D \rightarrow \infty$ we have to decide how the magnitudes in the problem scale with D , and in particular which quantities are kept fixed, *i.e.*, do not scale with D . An appropriate choice is one that results in a simple limit. We will keep the length r_0 fixed as $D \rightarrow \infty$.

Although we could set r_0 equal to one, the discussion is often clearer if we keep it explicit.

2.1 ‘Smallness’ of the horizon and a hierarchy of scales

Some of the properties of black holes at large D are not due to spacetime curvature but rather follow from elementary flat-space geometry (see appendix A). In particular, when D grows large, the area of the unit-radius sphere S^{D-2} ,

$$\Omega_{D-2} = \frac{2\pi^{(D-1)/2}}{\Gamma\left(\frac{D-1}{2}\right)}, \quad (2.3)$$

vanishes as

$$\Omega_{D-2} \rightarrow \frac{D}{\sqrt{2\pi}} \left(\frac{2\pi e}{D}\right)^{D/2} \rightarrow 0. \quad (2.4)$$

We may then say that these spheres becomes increasingly small at very large D , shrinking at a rate $\sim D^{-D/2}$. In particular, if we shoot a projectile at this unit-radius sphere, the impact cross section vanishes when $D \rightarrow \infty$, even if the projectile will hit the target whenever the impact parameter is < 1 .¹ This geometric effect will be present in all calculations of total cross sections at $D \rightarrow \infty$. The strong semifactorial suppression $\sim D^{-D/2}$ may sometimes hide effects that one is interested in, and in these cases it may be convenient to eliminate it by, *e.g.*, considering ratios of appropriate magnitudes.

There are other properties of the horizon, independent of this flat-space effect, which indicate that it is useful to think of the large D black hole as a very small object. The surface gravity on the horizon is

$$\kappa = \frac{D-3}{2r_0}, \quad (2.5)$$

which diverges as $D \rightarrow \infty$. Thus a length-scale arises associated to κ ,

$$\ell_\kappa = \kappa^{-1} \sim \frac{r_0}{D} \quad (2.6)$$

which is parametrically much smaller than the horizon radius r_0 . The intrinsic curvature gives essentially this same length. The Kretschmann scalar in the geometry (2.1) is

$$K = R_{\mu\nu\sigma\rho}R^{\mu\nu\sigma\rho} = \frac{(D-1)(D-2)^2(D-3)}{r^4} \left(\frac{r_0}{r}\right)^{2(D-3)} \quad (2.7)$$

so the characteristic curvature length of the horizon is

$$(K(r_0))^{-1/4} \rightarrow \frac{r_0}{D} \sim \ell_\kappa. \quad (2.8)$$

These short scales essentially reflect the large radial gradient of the gravitational potential near the horizon,

$$\partial_r f|_{r_0} \rightarrow \frac{D}{r_0}. \quad (2.9)$$

Since the classical theory of (1.1) is scale-free, one usually regards r_0 as the only length scale present in the solution (2.1), and in this respect it would not make sense to say that

¹The actual cross section of the unit S^{D-2} is $\sigma = \Omega_{D-3}/(D-2)$, whose dominant large D behavior is inversely semifactorial like that of Ω_{D-2} .

the black hole is small (compared to what?). But when D is very large we have identified a much shorter scale characterizing important aspects of the geometry.

Summarizing, there are two senses in which we can say that the black hole is effectively small. One is the vanishing area effect (2.4). The other is the appearance of the small length scale r_0/D , which we will see controls much of the classical black hole physics. Along this article we will develop and refine these ideas in much more detail.

2.2 Absence of interactions

Outside the horizon the gravitational potential $(r_0/r)^{D-3}$ vanishes exponentially fast in D . When $D \rightarrow \infty$ the lines of force are infinitely diluted in the infinite number of directions available, so there is no gravitational force outside the horizon. The horizon itself becomes a surface of infinite curvature. The spacetime of the black hole is then a flat geometry with a sphere cut off at the radius $r = r_0$. The area of this sphere is vanishingly small.

This implies that at $D \rightarrow \infty$ there is no force at all between two black holes. Multiple black hole solutions are obtained by simply cutting off spheres at different places in flat spacetime. Given this absence of interactions, and that these black holes present a vanishing cross section for colliding with each other, we may regard this as a system of ‘dust particles’.

The absence of a gravitational force, or equivalently the flatness of the metric outside the horizon, is also reflected in the fact that, for the solution (2.1), we have that

$$GM = \frac{(D-2)\Omega_{D-2}}{16\pi} r_0^{D-3} \quad (2.10)$$

vanishes as $D \rightarrow \infty$ due to the factor Ω_{D-2} . A caveat is now in order. The classical theory of (1.1) is in essence a purely geometric theory that only contains geometrical magnitudes, such as lengths and areas. Any other physical magnitudes, such as mass or angular momentum, which require the introduction of conversion constants such as G (absent from (1.1)), have only secondary meaning. Thus, G and M do not have any independent meaning in vacuum gravity. Nevertheless, with a view to coupling gravity to other matter systems, it may seem more appropriate to interpret (2.10) as saying that the gravitational coupling vanishes like

$$G \sim D^{-D/2} \rightarrow 0, \quad (2.11)$$

which suggests that the gravitational field becomes a free field at large D .

All large D scales in vacuum gravity must have an interpretation of purely geometric origin. GM can be regarded as a measure of how the extrinsic curvature of surfaces of constant r differs from the extrinsic curvature of the same surfaces when embedded in Minkowski space. At large D , this difference vanishes and hence $GM \rightarrow 0$. We may consider introducing a gravitational mass-length scale

$$\ell_M \sim (GM)^{1/(D-3)} \sim \frac{r_0}{\sqrt{D}}, \quad (2.12)$$

characterizing this effect. This length, however, can equally well be obtained from the horizon area,

$$\ell_A \sim A_H^{1/(D-2)} \sim \frac{r_0}{\sqrt{D}}. \quad (2.13)$$

It derives from the geometric effect discussed in eq. (2.4). The conceptual prevalence of geometric magnitudes must be borne in mind whenever we choose, for physical illustration, to frame our discussion in terms of non-geometric, secondary quantities.²

The picture of black holes as non-interacting dust also agrees well with other properties. The Bekenstein-Hawking entropy of the Schwarzschild black hole behaves like

$$S(M) \sim M^{\frac{D-2}{D-3}} \xrightarrow{D \rightarrow \infty} M. \quad (2.14)$$

In contrast to the situation at finite D , where $S \propto M^\alpha$ with $\alpha > 1$, the fact that $S \propto M$ means that there is no entropic gain in merging two black holes.³ Nor is there any entropic penalty in splitting a black hole in two (recall that the horizon becomes singular in the limit). This is a reflection of the absence of interactions noted above.

Consider now a black p -brane,

$$ds^2 = -f_p dt^2 + \sum_{i=1}^p dz_i^2 + f_p^{-1} dr^2 + r^2 d\Omega_{D-p-2}, \quad (2.15)$$

$$f_p = 1 - \left(\frac{r_0}{r}\right)^{D-p-3}. \quad (2.16)$$

This brane is characterized by an energy density ε and a pressure P along its worldvolume such that

$$P = -\frac{\varepsilon}{D-p-2}. \quad (2.17)$$

When $D \rightarrow \infty$ this pressure vanishes: the brane has a dust equation of state.

The instability of the dust brane to fragmentation in this limit is easy to establish. At any finite D , neutral black branes suffer from a Gregory-Laflamme instability to growing inhomogeneities along the worldvolume, and are expected to eventually break up [25]. The threshold mode at the onset of this instability has been studied at large D in [6, 7], with the result that perturbations with wavelength longer than

$$\lambda_c = \frac{2\pi r_0}{\sqrt{D}} (1 + O(D^{-1})) \quad (2.18)$$

are unstable. Thus, when $D \rightarrow \infty$ perturbations of arbitrarily short wavelength drive the break up of the brane. We will revisit this instability in more detail in section 7.

For black p -branes we can regard p as a parameter that can scale with D in different manners. The case of $p \sim O(D^0)$ has been discussed above. Another possibility is that

²Note that the quantum theory introduces the Planck length, which may be chosen to scale or not with D , see sec. 5.

³The shrinking effect of angular spheres may be eliminated by considering, *e.g.*, the ratio between initial and final entropies. This also eliminates the dependence on G and the Planck length.

$p \sim D$ in such a way that $n = D - p - 3$ remains finite, *i.e.*, we keep fixed the codimension of the brane instead of its worldvolume dimension. The gravitational field of these branes remains finite outside the horizon, and so does, too, their energy density and pressure. It seems appropriate to regard these black branes as belonging in a different sector of the theory than the infinitely localized ones we are considering so far, as they cannot be produced through processes involving a finite number of the latter. Their dynamics appears to be dominated by the degrees of freedom of a Kaluza-Klein reduction down to $n + 3$ dimensions. Except for a brief mention in the next subsection, we will not consider these branes in the remainder.

2.3 Other black holes: rotation and other topologies

When rotation is present in any $D \geq 4$ there are large classes of black hole solutions with many possible horizon topologies. Although the entire space of solutions has not been fully mapped, we can argue that the limit $D \rightarrow \infty$ results in configurations with singular horizons and flat space outside them. Equilibrium horizons are equipotential surfaces, and at large D the gravitational potential falls off steeply in the transverse direction away from them. If we take the limit $D \rightarrow \infty$ in such a way that the length scales that characterize the horizon remain finite, then the potential will drop infinitely fast outside the horizon. A possible concern is that in $D \geq 4$ there are horizons that are much more elongated in some directions than in others, and in these cases the gravitational potential close to the horizon falls off more slowly than at asymptotically large distances. Nevertheless, if the limit $D \rightarrow \infty$ is taken keeping the horizon length scales finite, the region where this slower fall off occurs shrinks and disappears in the limit. We can confirm all these features by studying explicit known solutions.

Myers-Perry black holes. Each independent rotation introduces a new length parameter a . Even if this parameter is usually regarded as the ratio of angular momentum to mass, as we discussed earlier the length a is a more basic, purely geometrical quantity. We take these parameters a to scale in such a manner as to preserve finiteness of the metric.

Let us take the limit $D \rightarrow \infty$ for Myers-Perry black holes with several non-zero rotation parameters. We find no important distinction between the even- or odd-dimensional cases, so for definiteness we take odd D . The solution is [26]

$$ds^2 = -dt^2 + (r^2 + a_i^2)(d\mu_i^2 + \mu_i^2 d\varphi_i^2) + \frac{r^2 r_0^{D-3}}{\Pi F} (dt + a_i \mu_i^2 d\varphi_i)^2 + \frac{\Pi F}{\Pi - r^2 r_0^{D-3}} dr^2, \quad (2.19)$$

where summation over $i = 1, \dots, \frac{D-1}{2}$ is assumed, direction cosines satisfy $\mu_i^2 = 1$, and

$$F = 1 - \frac{a_i^2 \mu_i^2}{r^2 + a_i^2}, \quad \Pi = \prod_{i=1}^{(D-1)/2} (r^2 + a_i^2). \quad (2.20)$$

When $r_0 = 0$ the metric

$$ds^2 = -dt^2 + (r^2 + a_i^2)(d\mu_i^2 + \mu_i^2 d\varphi_i^2) + Fdr^2 \quad (2.21)$$

describes flat space in ellipsoidal coordinates. When $r_0 > 0$, the horizon is at $r = r_H$ such that $r_H^2 r_0^{D-3} = \Pi(r_H)$. Let k be the number of non-zero rotation parameters a_i , and for simplicity of illustration set them all equal to a . Then we have

$$\frac{r^2 r_0^{D-3}}{\Pi} = \left(\frac{r_0}{r}\right)^{D-3} \left(1 + \frac{a^2}{r^2}\right)^{-k}, \quad (2.22)$$

so r_H is found by solving

$$\frac{r_0}{r_H} = \left(1 + \frac{a^2}{r_H^2}\right)^{\frac{k}{D-3}}. \quad (2.23)$$

If we keep k fixed when $D \rightarrow \infty$ then $r_H \rightarrow r_0$, and $r^2 r_0^{D-3}/\Pi$ clearly vanishes for $r > r_0$: the metric becomes flat spacetime everywhere outside the horizon.

If instead the number k of non-zero spins grows with D such that $m = \frac{D-1}{2} - k$ remains fixed, then in the limit $D \rightarrow \infty$ eq. (2.23) becomes

$$\frac{r_0}{r_H} = \left(1 + \frac{a^2}{r_H^2}\right)^{1/2} \Rightarrow r_H = \sqrt{r_0^2 - a^2}. \quad (2.24)$$

So $r_H \rightarrow r_0$, but still

$$\frac{r^2 r_0^{D-3}}{\Pi} \rightarrow \left(\frac{r_H^2 + a^2}{r^2 + a^2}\right)^{D/2} \quad (2.25)$$

vanishes, and thus leaves flat spacetime, at any $r > r_H$ when $D \rightarrow \infty$. This is the case even when $r_0 \simeq a$, in which case r_H is very small, the horizon can be highly pancaked (at least if some spins vanish), and $r_H \ll a$, which can be regarded as an ultraspinning limit [27]. The main point to note is that, in spite of the fact that at finite D there is a region very close to the black hole where the potential falls off like $r^{-2(m-1)}$ (instead of r^{3-D}), the radial extent of this region vanishes in the limit $D \rightarrow \infty$ when we keep r_0 and a fixed.

Summarizing, in the limit $D \rightarrow \infty$ the gravitational field vanishes completely outside the horizon, and the effect of $a \neq 0$ is that the surface in (2.21) that is cut off at $r = r_0$ is not a sphere but an ellipsoid.

The product GM of the solution vanishes in the limit for the same reason as in the static case. The angular momentum in gravitational units, GJ , also vanishes, which seems natural if we interpret that G vanishes. It is interesting that the ratio

$$\frac{J}{M} = \frac{2a}{D-2}, \quad (2.26)$$

which is not suppressed by factors of Ω_{D-2} , approaches zero. On the other hand the angular velocity on the horizon

$$\Omega_H = \frac{a}{r_H^2 + a^2} \quad (2.27)$$

remains finite when $D \rightarrow \infty$, even though no rotational dragging is felt anywhere outside $r = r_H$. The surface gravity in the singly-rotating case,

$$\kappa = \frac{1}{2} \left(\frac{2r_H}{r_H^2 + a^2} + \frac{D-5}{r_H} \right) \quad (2.28)$$

diverges like it did in the static case, but its minimum at

$$\frac{a}{r_H} = \sqrt{\frac{D-3}{D-5}} \quad (2.29)$$

remains finite as $D \rightarrow \infty$. This suggests that the value $a/r_H = 1$ separates the regimes in which rotating black holes at large D are stable or unstable to axisymmetric perturbations of the type discussed in [27].

Blackfolds. Other types of rotating black holes are known to exist in $D \geq 5$. Exact analytical solutions have only been found in five dimensions, but approximate solutions are known for black rings and many other black holes in arbitrary $D \geq 5$ [28, 29]. These are built by smoothly bending black branes, and are referred to as blackfolds. We can infer their large D limits from the properties of black p -branes.

It is easy to see that a blackfold constructed out of a black p -brane, with p fixed as $D \rightarrow \infty$, becomes a ‘dust- p -fold’ as $D \rightarrow \infty$ when we keep finite the appropriate length parameters that determine its geometry (*e.g.*, horizon thickness and worldvolume curvature radius). For instance, for a black ring with horizon $S^1 \times S^{D-3}$ we keep the radius of the S^{D-3} and of the S^1 fixed as $D \rightarrow \infty$, and find a ‘ring of dust’ with vanishing rotation velocity and a flat metric outside the singular horizon.

We may also have black p -folds for which p diverges but $n = D - p - 3$ remains fixed as $D \rightarrow \infty$. We are interested in the cases for which the gravitational potential beyond some distance r_c remains bounded above and behaves, at finite D , like $(r_c/r)^{D-3}$. Then when $D \rightarrow \infty$ it will vanish for $r > r_c$. While it might seem possible that the radius r_c lies at a finite distance outside the horizon, the evidence we have found from the Myers-Perry solutions, which include blackfolds in this class, confirms our expectation that the spacetime becomes flat outside the horizon. For these objects, GM must vanish. A simple example besides the Myers-Perry solutions are homogeneous black p -folds with volume V_{D-n-3} , for which [29]

$$16\pi GM = (D-2)V_{D-n-3}\Omega_{n+1}r_0^n. \quad (2.30)$$

We are keeping n and r_0 fixed. Now, in the case of *e.g.*, a spherical blackfold, the volume $R^{D-n-3}\Omega_{D-n-3}$, and with it GM , vanishes due to $\Omega_{D-n-3} \rightarrow 0$. So blackfolds of this type appear to conform to our general picture. There can also be blackfolds for which V_{D-n-3} does not vanish when $D \rightarrow \infty$, for example toroidal blackfolds with $V_{D-n-3} = L^{D-n-3}$ with L fixed. Their mass-length (2.12)

$$\ell_M \sim L^{\frac{D-n-3}{D-3}} r_0^{\frac{n}{D-3}} (D-2)^{\frac{1}{D-3}} \rightarrow L \quad (2.31)$$

remains finite. It is doubtful that these objects can be sensibly defined in the limit $D \rightarrow \infty$: at large distances their metric coefficients cannot be finite. If a suitable limit existed, they would form a different, infinitely more massive sector of the theory, similar to the black p -branes discussed at the end of sec. 2.2. In this article we will not consider them any further.

2.4 Charge

The gravitational effect of the electric field in a Reissner-Nordstrom black hole is characterized by a charge-radius r_Q , related to the charge Q by [26]

$$Q = \sqrt{\frac{(D-2)(D-3)}{8\pi G}} r_Q^{D-3}. \quad (2.32)$$

This radius appears in the metric in the form $(r_Q/r)^{2(D-3)}$. If, as may be natural in this context, we assume that we keep r_Q fixed, then the gravitational effect of the charge vanishes at distances $r > r_Q$. Note that Q is measured in units of the gauge coupling (the electron charge). So if G is chosen to scale like (2.11) (to keep the mass fixed, for fixed r_0), then we may keep both r_Q and the charge Q fixed if the gauge coupling is made to vanish like $D^{-D/4}$.

Similarly, the effect of p -form charges (with p not scaling with D), which can be carried by black p -branes or by black holes with non-spherical topologies [30, 31, 32], vanishes in the directions transverse to the brane if we keep their charge-radius fixed. However, a p -form charge forbids the break up of the brane in the p directions parallel to the worldvolume. In these cases the equation of state of the brane does not become dust-like. For instance, for dilatonic p -branes in the limit $D \rightarrow \infty$ one finds

$$P = -\frac{N \sinh^2 \alpha}{1 + N \sinh^2 \alpha} \varepsilon, \quad (2.33)$$

where α is the charge-boost parameter (which remains fixed as $D \rightarrow \infty$ if the charge radius is fixed) and N determines the dilaton coupling (see *e.g.*, [32]). The field nevertheless vanishes outside the horizon.

2.5 Large D in Anti-deSitter

The cosmological constant Λ in Anti-deSitter spacetime introduces a curvature length scale.⁴ In the limit $D \rightarrow \infty$, instead of fixing Λ it is sensible to keep

$$L = \sqrt{\frac{(D-1)(D-2)}{|\Lambda|}} \sim \frac{D}{\sqrt{|\Lambda|}}, \quad (2.34)$$

since this is the length that appears in the metric. If we kept Λ fixed, we would have $L \rightarrow \infty$ and the effect of the cosmological constant would disappear from the geometry.

⁴The first part of this discussion applies also to de Sitter spacetime and to Schwarzschild-de Sitter black holes away from the Nariai limit.

Again, we focus on the simplest black hole solution, which has the same form as (2.1) but with [33]

$$f(r) = 1 - \left(\frac{r_0}{r}\right)^{D-3} + \frac{r^2}{L^2}. \quad (2.35)$$

The event horizon is not at $r = r_0$ but rather at $r_H > r_0$, the real positive radius where $f(r_H) = 0$. At large D ,

$$r_H = r_0 \left(1 - \frac{1}{D} \ln \left(1 + \frac{r_0^2}{L^2}\right) + O(D^{-2})\right). \quad (2.36)$$

Thus, $r_H \rightarrow r_0$ when $D \rightarrow \infty$. Like in flat space, in this limit the gravitational effect of the black hole outside this horizon vanishes. Black holes are again non-interacting particles, now in Anti-deSitter spacetime. However, although their area vanishes due to $\Omega_{D-2} \rightarrow 0$, these black holes are not always ‘small AdS black holes’, since r_H can still be either smaller or larger than L . Their temperature is

$$T = \frac{(D-1)r_H^2 + (D-3)L^2}{4\pi L^2 r_H} \quad (2.37)$$

so

$$T \rightarrow \frac{D}{4\pi r_0} \left(1 + \frac{r_0^2}{L^2}\right) + O(D^0). \quad (2.38)$$

Although this diverges when $D \rightarrow \infty$ (like in flat spacetime), as a function of r_0 this temperature reaches a minimum at $r_0 = L$. We may then regard black holes as small or large according to whether $r_0 < L$ or $r_0 > L$. We see in (2.36), (2.38) that the presence of L modifies the large- D short scales, in particular the surface gravity length is

$$\ell_\kappa \sim \frac{r_0 L^2}{D(r_0^2 + L^2)}, \quad (2.39)$$

and its dependence on r_0 is rather different in the two regimes $r_0 \lesseqgtr L$.

The shrinking effect of the Euclidean time circle and of the area of the spheres S^{D-2} as $D \rightarrow \infty$ may be, if convenient, factored out by, *e.g.*, dividing T by D , and dividing extensive thermodynamic quantities by Ω_{D-2} . For instance, the Euclidean action of the black hole spacetime vanishes, both because of the factor Ω_{D-2} and because of the shrinking Euclidean time circle. In this case there is no trace of the Hawking-Page transition at $D \rightarrow \infty$. However, if we introduce a rescaled free energy

$$\hat{F} = \frac{16\pi G}{\Omega_{D-2} L^{D-3}} F = \left(\frac{r_H}{L}\right)^{D-3} \left(1 - \frac{r_H^2}{L^2}\right), \quad (2.40)$$

then the Hawking-Page transition at which \hat{F} changes sign, is apparent at $r_H = L$, although extremely abrupt: at $D \rightarrow \infty$ this free energy changes from $-\infty$ for $r_H > L$, to 0^+ for $r_H < L$. Another way to avoid these divergences is to consider ratios between extensive quantities.

The limit of very large AdS black holes yields planar black branes in Poincaré AdS. These black branes have a conformal equation of state $P = \varepsilon/(D-1)$, so in the limit

$D \rightarrow \infty$ they behave again like ‘dust’ branes, which are marginally stable to longitudinal fluctuations, with empty AdS spacetime outside them. In section 7.5 we briefly revisit these branes.

In summary, all our knowledge about higher-dimensional black holes points to the conclusion that even when the effects of rotation, different horizon topologies, charge, or cosmological constant, are accounted for, the limit $D \rightarrow \infty$ consists of configurations of objects with flat (or AdS) spacetime outside their singular horizons. We return now to extract more information from the basic solution (2.1).

3 Sphere of influence

While in the limit $D \rightarrow \infty$ the gravitational field vanishes at all $r > r_0$, when D is large but finite there is a small region around the horizon where the black hole exerts its gravitational influence. More precisely, outside the horizon the gravitational potential is still appreciable, *i.e.*,

$$\left(\frac{r_0}{r}\right)^{D-3} = O(D^0), \quad (3.1)$$

within the region

$$r - r_0 \lesssim \frac{r_0}{D} + O(D^{-2}), \quad (3.2)$$

while it vanishes exponentially fast in D outside this range.

For some observables this ‘sphere of influence’, characterizing the degree to which a phenomenon is localized close to the horizon, may extend out to a further radius. Typically this is due to radial derivatives of $f(r)$, each of which brings in a factor $\sim D$. In general, the relevant result is that, for $r > r_0$,

$$D^b \left(\frac{r_0}{r}\right)^D = O(D^0) \quad \Leftrightarrow \quad r - r_0 \lesssim \frac{r_0}{D} (a + b \ln D) + O(D^{-2}), \quad (3.3)$$

where a, b are D -independent numbers. For instance, the effects of the gravitational force $\partial_r f$ have a range of this form with $b = 1$. We see this in the acceleration of an observer at constant r in (2.1),

$$a = \frac{D-3}{2r_0\sqrt{f(r)}} \left(\frac{r_0}{r}\right)^{D-2} \xrightarrow{D \rightarrow \infty} \frac{D}{2r_0} \left(\frac{r_0}{r}\right)^D, \quad (3.4)$$

which has a range

$$r - r_0 \lesssim \frac{r_0}{D} \ln D + O(D^{-2}). \quad (3.5)$$

An example with $b = 2$ is the Kretschmann scalar (2.7), which is of order one in the region

$$r - r_0 \lesssim \frac{2r_0}{D} \ln D + O(D^{-2}). \quad (3.6)$$

The scattering of light rays thrown towards the black hole (2.1) provides another illustration. These rays will be absorbed if the impact parameter b is smaller than the critical value [34]

$$b_c = \left(\frac{D-1}{2} \right)^{1/(D-3)} \sqrt{\frac{D-1}{D-3}} r_0. \quad (3.7)$$

As $D \rightarrow \infty$ this gives $b_c \rightarrow r_0$. Light rays that pass with $b > r_0$ suffer no deflection: it is infinitely difficult to catch a line of force that pulls towards the black hole. At finite but large D the photon sphere of influence is

$$b_c = r_0 \left(1 + \frac{1 + \ln(D/2)}{D} + O(D^{-2}) \right). \quad (3.8)$$

The photon absorption cross section

$$\sigma = \frac{\Omega_{D-3}}{D-2} b_c^{D-2} \quad (3.9)$$

vanishes as $D^{-D/2}$, as already discussed. For the rotating black hole (2.19), the critical impact parameter for light rays in the plane $\mu_k = 1$ asymptotes to $b_c \rightarrow \sqrt{r_0^2 + a_k^2}$, which is precisely the radius of the circle at $r = r_0$ in this plane in the limiting flat geometry (2.21).

3.1 Quasinormal modes

Quasinormal modes characterize the black hole's own dynamics. It is natural to expect that they are localized close to the sphere of influence and controlled by the scale r_0/D . This is actually the case. At large D the quasinormal frequencies can be estimated or computed (see [35, 36, 13] and section 6 below) with the result that for either scalar, vector or tensor perturbations,

$$\text{Re } \omega_{\text{QN}} \sim \frac{D}{r_0}, \quad (3.10)$$

at least when the angular momentum and overtone numbers are $\ll D^2$. In the WKB approximation these quasinormal modes can be regarded as localized close to the circular photon orbit at

$$\begin{aligned} r_{ph} &= \left(\frac{D-1}{2} \right)^{1/(D-3)} r_0 \\ &= r_0 \left(1 + \frac{\ln(D/2)}{D} \right) + O(D^{-2}). \end{aligned} \quad (3.11)$$

The imaginary part of ω_{QN} is suppressed at large D relative to the real part, which may be related to the apparent ease with which black holes can fragment in this limit.

3.2 Across the horizon, a small interior

In the limit $D \rightarrow \infty$ a particle that falls in the black hole encounters a singularity at $r = r_0$ where its trajectory comes to an end. However, for large but finite D the horizon is a non-singular place and we can ask how long it takes for the particle to reach the singularity at $r = 0$ — *i.e.*, what scale controls the internal size of the black hole.

Taking for simplicity a particle that starts at rest at infinity in a radial trajectory, the proper time elapsed between the moment it crosses the radius $r = R$ until it reaches the singularity is

$$t_{sing} = \int_0^R dr \left(\frac{r}{r_0} \right)^{\frac{D-3}{2}} = \frac{2r_0}{D-1} \left(\frac{R}{r_0} \right)^{\frac{D-1}{2}}. \quad (3.12)$$

The two factors in this result each have a different origin. In the large D limit the particle takes a time that diverges exponentially with D to go from any finite distance outside the sphere of influence until it reaches this region, where $(R/r_0)^D \sim 1$; this is just a reflection of the very small gravitational force outside this sphere. From the moment when the particle enters this region until it reaches the singularity, the time (3.12) that passes is

$$t_{sing} \simeq \frac{2r_0}{D} + O(D^{-2}), \quad (3.13)$$

i.e., a very short time, determined once again by the scale r_0/D . Most of this time is spent in the sphere of influence, which now includes an inner region $r_0 - r \lesssim r_0/D$. After that, the singularity is reached exponentially fast in D . Eq. (3.13) gives a sense in which we can regard the black hole interior as small.

4 Classical radiation from black hole interactions

The absence of a gravitational field inbetween two or more black holes implies that, when they move in the presence of one another, no gravitational radiation is emitted. Below we verify that this is consistent with the large D limit of several previously studied processes, but there is an effect that remains in phenomena that probe very short lengths $\lesssim r_0/D$.

4.1 Black hole collisions

For simplicity we study collisions among black holes of equal size. It is clear that when $D \rightarrow \infty$ two black holes thrown towards one another will not be deflected from their straight paths unless the impact parameter is $\leq r_0$. An often studied case is the ultrarelativistic limit, *i.e.*, the collision of two Aichelburg-Sexl shockwave solutions. It is immediate to see that at $D \rightarrow \infty$ these solutions become trivially flat outside a singularity at the center of the shockwave plane — away from this point, the shock itself disappears. So, in this limit, for any collision course that is not exactly head-on, we conclude, unshockingly, that the particles simply fly by each other, with no emission of radiation.

Put now the black holes in a head-on collision course. Collision is unavoidable, but will there be any radiation emission? If the black holes start towards each other with infinitesimal velocities, then our argument about the entropy in a merger in sec. 2.2 tells us that no radiation will be produced when they merge. More generally, if they move towards each other with initial velocities $\pm v$, then the area theorem imposes an upper bound on the ratio of the radiated energy to the initial energy [37] which, when $D \rightarrow \infty$, is⁵

$$\epsilon(v) = \frac{E_{rad}}{E_{in}} \leq 1 - \sqrt{1 - v^2}. \quad (4.1)$$

As $v \rightarrow 0$ we recover $\epsilon \rightarrow 0$, *i.e.*, no radiation, but for $v > 0$ there is the possibility that radiation is produced. This indicates that kinetic energy, but not any rest mass of the black holes, can be converted into radiation.

We may expect that the actual ϵ is maximized in ultrarelativistic collisions and in fact when $v \rightarrow 1$ the condition (4.1) imposes no constraint. For shockwave collisions a more stringent bound on ϵ can be obtained from the area of the apparent horizon at the moment that the shockwaves meet [38, 12]. When $D \rightarrow \infty$ this bound becomes

$$\epsilon_{\text{shock}} \leq \frac{1}{2}. \quad (4.2)$$

According to refs. [18, 19], this bound is actually saturated, and thus gravitational radiation is indeed produced at $D \rightarrow \infty$. This might appear to run against the picture of $D \rightarrow \infty$ black holes as non-interacting dust particles, but there is a plausible interpretation for this result. A head-on collision is an extremely fine-tuned process (even more so at $D \rightarrow \infty$ where the cross section vanishes) which can excite dynamics at infinitely short distances involving modes of infinitely high frequency, such as the quasinormal modes with $\omega \sim D/r_0$, which are localized in the region (3.11) very near the black holes. At large D these modes can get excited if (and only if) very short scales $\sim r_0/D$ are probed.

More precisely, the emission of radiation comes with a factor $\sim \omega^D$ from the frequency-volume available to radiation. If the characteristic length of modes that are radiated is ℓ , then the process will be governed by a factor $(\omega\ell)^D$. Emission will be completely shut off when the frequencies that can be excited in a process are $\omega < \ell^{-1}$, but it may remain appreciable as $D \rightarrow \infty$ when $\omega \sim \ell$, even if ℓ vanishes in this limit. In the following we find evidence that this effect is indeed present, and moreover that the relevant scale is $\ell \sim r_0/D$, *i.e.*, that of typical quasinormal modes.⁶

Ref. [39] estimated the amount of radiation produced in black hole collisions in the ‘instantaneous collision approximation’ (which may in fact become more accurate as D grows). At moderate (not ultrarelativistic) initial velocities, and ignoring D -independent

⁵Even if the individual masses and areas vanish due to the shrinking factors of Ω_{D-2} , these cancel out in this ratio. Also all factors of G cancel, so this is a quantity that can be defined with reference to purely geometric quantities.

⁶The fact that the number of graviton polarizations grows like D^2 does not seem to play more than a subleading a role, negligible for the previous argument.

numbers, the leading large D emission per solid angle is⁷

$$\frac{dE_{rad}}{d\Omega} \sim GM^2 \omega_m^{D-3}, \quad (4.3)$$

where ω_m is a (physical) cutoff in the frequencies that are radiated. Integrating over all angular directions, the ratio of the total radiated energy to the black holes' mass is

$$\epsilon \simeq \frac{E_{rad}}{2M} \sim \frac{\Omega_{D-2}}{M} \frac{dE_{rad}}{d\Omega} \sim \left(\frac{\omega_m r_0}{D} \right)^D \quad (4.4)$$

(we have used (2.12)). If the frequency cutoff were $\omega_m \sim r_0^{-1}$ then no radiation would be emitted when $D \rightarrow \infty$. But precisely at the frequencies $\omega_m \sim D/r_0$ there is a big enhancement in the emission of radiation.

Our next example provides another instance in which there is a possibility of producing radiation by exciting frequencies $\sim D/r_0$. It is worth stressing that neither of these calculations involve a quasinormal mode study, nor indeed any perturbation analysis of the black hole spacetime (2.1). We find remarkable the consistent appearance of this scale.

4.2 Orbiting black holes

The radiating power from two black holes, each with Schwarzschild radius r_0 and mass M , orbiting around each other at a distance l and with orbital frequency ω , tends at large D to⁸

$$\frac{dE_{rad}}{dt} \sim \Omega_{D-2} GM^2 l^4 \omega^{D+2} \quad (4.5)$$

(again up to D -independent numerical factors) [39]. The fraction of the system's energy emitted per orbit is

$$\epsilon \simeq \frac{\pi}{M\omega} \frac{dE_{rad}}{dt} \sim \left(\frac{\sqrt{D}l}{r_0} \right)^4 \left(\frac{\omega r_0}{D} \right)^D. \quad (4.6)$$

If the black holes follow Keplerian orbits with $l > r_0$ then

$$\omega \sim \sqrt{\frac{GM}{l^{D-1}}} \sim \frac{1}{l} \left(\frac{r_0}{\sqrt{D}l} \right)^{D/2} \quad (4.7)$$

vanishes as D grows, since their mutual attraction becomes increasingly weaker (this also justifies the simplifications made in deriving (4.6), although note that the orbits are unstable). This does fit the picture of non-interacting, non-radiating particles.

However, let us push the argument further and consider that the black holes follow circular trajectories under an external force (whose gravitational effect we neglect; we proceed even it is unclear how sensible this is), so that ω is independent of the black hole masses and their separation. The dominant factor in (4.6) at large D is $(\omega r_0/D)^D$. So when the orbital frequency is $\omega \sim D/r_0$, *i.e.*, when the motion is so fast that it is capable

⁷The dependence on dimensionful parameters in this equation can be easily worked out from generic considerations. But note that we are also accounting for the dominant D -dependent dimensionless factors.

⁸See footnote 7.

of exciting the quasinormal modes of the black hole, radiation is possible as $D \rightarrow \infty$. In this regime the approximations made in deriving (4.6) certainly cease to be justified, but still we can observe how the excitation of the very high-frequency modes in the thin region near the horizon may result in radiation that survives the limit $D \rightarrow \infty$.

The themes of this section will reappear in sec. 6, where we confirm this picture of the interaction of the black hole with classical waves.

5 Quantum effects

We do not study quantum gravitational effects in any detail but merely make some elementary remarks.

Since the curvature (2.7) at the horizon grows unbounded at large D , one can expect a breakdown of the semiclassical gravitational effective theory in the close vicinity of the horizon. The same effect is seen in the black hole temperature,

$$T_H = \frac{D-3}{4\pi r_0}. \quad (5.1)$$

As $D \rightarrow \infty$, T_H reaches arbitrarily high values eventually hitting the Planck scale. This occurs even when r_0 is larger than the Planck length L_{Planck} , because the scale controlling the curvature and temperature is not r_0 but r_0/D . In this reasoning we are assuming that the Planck scale does not scale with D . If, instead, we choose to scale it as $L_{\text{Planck}} \sim D^{-1}$ (and so $E_{\text{Planck}} \sim D$), *e.g.*, $L_{\text{Planck}} = \hat{L}_{\text{Planck}}/D$, then quantum gravitational effects might be suppressed when $r_0 \gg \hat{L}_{\text{Planck}}$. This type of scaling, therefore, might seem more appropriate for the study of semiclassical effects.

The situation, however, is subtle. Consider Hawking radiation at large D , which was studied in ref. [16]. One might expect that the typical frequency of Hawking quanta should be of the order of $T_H \sim D/r_0$. However, the actual typical frequencies are much larger. The reason is the huge increase in the phase space available to high-frequency quanta at large D (already encountered in sec. 4), which shifts the radiation spectrum towards frequencies much larger than T_H . The number density distribution of quanta at temperature T is

$$n(\omega)d\omega = \Omega_{D-2} \frac{\omega^{D-2}d\omega}{e^{\omega/T} - 1}, \quad (5.2)$$

with the factor Ω_{D-2} coming from the angular integration in momentum-space. At fixed but large D , this density peaks at [16]

$$\omega = DT (1 + O(e^{-D})) \gg T. \quad (5.3)$$

Then, for a black hole the typical frequency of Hawking quanta is

$$\omega_H \simeq DT_H \simeq \frac{D^2}{4\pi r_0}. \quad (5.4)$$

We see that even if we scaled $E_{\text{Planck}} \sim D$, we would still have $\omega_H/E_{\text{Planck}} \sim D \gg 1$: Hawking quanta would still reach superPlanckian energies. It is unclear whether a stronger scaling of the Planck length with D would be useful.

Thus the black hole is a very *large* quantum radiator, whose radius ($\sim r_0$) and typical classical vibrational wavelengths ($\sim r_0/D$) are much longer than the wavelengths it radiates quantum mechanically ($\sim r_0/D^2$). In this respect it is interesting that, even if phase space integrals receive suppressing factors of Ω_{D-2} from angular integrals (from both momentum and position space), these are offset by the growth $\sim \omega^{D-2}$ of volume in radial (frequency) directions. The number density (5.2) at the peak frequency (5.4) behaves like

$$n(\omega_H) \sim \Omega_{D-2}(T_H D)^{D-2} \sim D^{3D/2}. \quad (5.5)$$

Then, the total Hawking flux, even if radiated by an object of vanishingly small area $A_H \sim D^{-D/2}$, still shows factorial growth $\sim D^D$. This enhancement is due to the fact that $T_H \sim D$.⁹ For practical applications of the large D limit, the ultrashort wavelength of Hawking radiation can be a bonus since it implies that the geometric optics approximation for graybody factors applies very accurately [16].

It would be interesting to investigate whether the black hole information problem can be sensibly formulated in the $1/D$ expansion. Let us mention, among the potentially relevant factors, that at $D \rightarrow \infty$ the singular horizon (which has zero area) perfectly reflects radiation of any finite frequency. This might seem to prevent information from being lost across the horizon (although it might also be destroyed there), but on the other hand Hawking pairs come out at infinite frequency. For very large but finite D the very short time (3.12) available for measurement for observers who cross the horizon might facilitate the consistency of a form of black hole complementarity, but the extremely fast evaporation rate compresses enormously *all* the timescales involved. It is then unclear without a more careful investigation whether these are positive or negative features for making this a useful approach.

6 Large D effective theory: scalar wave absorption

Up to this point we have been mostly drawing consequences from the limit $D \rightarrow \infty$ in processes that had already been calculated at finite D . We have gathered ample evidence that a consistent picture emerges. Now we apply the large D expansion to problems that have not been fully solved previously in analytic form. The main idea that simplifies their study is the following.

6.1 Near and far regions

The gravitational field is strongly localized within a region close to the horizon characterized by the scale r_0/D . This is a length that at large D is widely separate from the radius

⁹See footnote 6.

r_0 , so we can define two distinct but overlapping regions in the geometry:

$$\begin{aligned} \text{near region : } r - r_0 &\ll r_0, \\ \text{far region : } r - r_0 &\gg \frac{r_0}{D}. \end{aligned} \quad (6.1)$$

Equivalently, introducing the variable $R \equiv (r/r_0)^D$ they can be characterized as

$$\begin{aligned} \text{near region : } \ln R &\ll D, \\ \text{far region : } \ln R &\gg 1. \end{aligned} \quad (6.2)$$

The far region, where the geometry is effectively flat, excludes the sphere of influence (3.2). The latter is part of the near region,¹⁰ which extends into an

$$\text{overlap region : } \frac{r_0}{D} \ll r - r_0 \ll r_0, \quad i.e., \quad 1 \ll \ln R \ll D, \quad (6.3)$$

very close to the horizon, where it smoothly connects to the far region. Then, the study of *any* phenomenon that takes place in this geometry lends itself naturally to the method of matched asymptotic expansions (first used in this context in [7]). If we manage to solve the field equations in the near region, with regularity conditions imposed on the horizon, then this solution will provide boundary conditions for the far field by requiring that the fields match where they overlap.

6.2 Massless scalar wave equation

We study massless scalar field propagation in the black hole background (2.1). Throughout this section it will be slightly convenient to work with the parameter

$$n = D - 3 \quad (6.4)$$

instead of D . At large D they are of course equivalent.

We study the wave equation

$$\square \Psi = 0 \quad (6.5)$$

in the background (2.1). We set

$$\Psi = e^{-i\omega t} \psi_{\omega l}(r) Y_{n+1}^{(l)}(\Omega), \quad (6.6)$$

where $Y_{n+1}^{(l)}(\Omega)$ are spherical harmonics on S^{n+1} , and henceforth we drop the mode indices from ψ . The equation becomes

$$\frac{1}{r^{n+1}} \frac{d}{dr} \left(r^{n+1} f(r) \frac{d}{dr} \psi \right) + \frac{\omega^2}{f(r)} \psi - \frac{l(l+n)}{r^2} \psi = 0. \quad (6.7)$$

It is conventional to write this as an equation for

$$\phi(r) = r^{(n+1)/2} \psi(r) \quad (6.8)$$

¹⁰Incidentally, the near region retains more features than a Rindler horizon.

in the form

$$\frac{d^2\phi}{dr_*^2} + (\omega^2 - V(r_*))\phi = 0, \quad (6.9)$$

where the tortoise coordinate defined by $dr_* = dr/f(r)$ is given in terms of a hypergeometric function,

$$r_* = {}_2F_1\left(-\frac{1}{n}, 1, \frac{n-1}{n}; \left(\frac{r_0}{r}\right)^n\right) r, \quad (6.10)$$

and

$$V(r_*) = \frac{f(r)}{4r^2} \left((2l+n)^2 - 1 + (n+1)^2 \left(\frac{r_0}{r}\right)^n \right) \quad (6.11)$$

is the Regge-Wheeler potential for these perturbations.

At large n this potential scales like n^2 . In order to capture physics of interest we introduce

$$\hat{\omega} = \frac{\omega}{n}, \quad \hat{l} = \frac{l}{n} \quad (6.12)$$

and consider $\hat{\omega}$ and \hat{l} as $O(1)$ quantities. Now when n is large the equation becomes

$$\frac{d^2\phi}{dr_*^2} + n^2 (\hat{\omega}^2 - \hat{V}(r_*))\phi = 0, \quad (6.13)$$

with

$$\hat{V}(r_*) = \frac{f(r)}{4r^2} \left((2\hat{l}+1)^2 + \left(\frac{r_0}{r}\right)^n \right). \quad (6.14)$$

This potential vanishes on the horizon at $r_* \rightarrow -\infty$ and in the asymptotic region at $r_* \rightarrow +\infty$. It has a maximum at

$$r = r_{\max} = r_0 \left(2n \frac{\hat{l}(\hat{l}+1)}{(2\hat{l}+1)^2} + O(n^0) \right)^{1/n}. \quad (6.15)$$

When $\hat{l} \gg 1$ this is

$$r_{\max} = r_0 \left(1 + \frac{\ln(n/2)}{n} \right) + O(n^{-2}), \quad (6.16)$$

which reproduces the radius of the circular photon orbit (3.11). The maximum of the potential, corresponding to critical scattering at the threshold of absorption, occurs for the frequency $\hat{\omega} = \omega_c$, with

$$\omega_c r_0 = \hat{l} + \frac{1}{2} + O(n^{-1}). \quad (6.17)$$

This gives the real part of the quasinormal mode frequency (3.10) in the WKB approximation. The critical impact parameter $b_c = \hat{l}/\omega_c$ at $\hat{l} \gg 1$ reproduces the geometric optics result (3.9) at large n . This critical frequency will play a central role in the problem.

When $n \rightarrow \infty$ this potential becomes extremely simple: for $r_* > r_{\max}$ (where $r_* = r$) we recover the flat space potential with only a centrifugal barrier. For $r_* < r_{\max}$ the potential vanishes exponentially quickly in n . So the limiting form of the potential is

$$\hat{V}(r_*) \rightarrow \frac{\omega_c^2 r_0^2}{r_*^2} \Theta(r_* - r_0). \quad (6.18)$$

We recognize here two of the main running themes of this article. First, waves outside the black hole propagate in a flat space potential. Its height $V(r_{\max}) \sim n^2$ becomes infinite when $n \rightarrow \infty$, so in this limit excitations of frequency $\omega = O(n^0)$ are not absorbed at all: this radiation does not interact with the black hole. Second, waves of frequency $\omega \gtrsim n/r_0$ can penetrate the barrier and probe the dynamics near the horizon of the black hole.

Problems of field propagation are characterized by the field amplitudes at infinity and at the horizon,

$$\phi \sim \begin{cases} A_l^{\text{in}}(\omega) (e^{-i\omega r_*} + R_l(\omega) e^{i\omega r_*}) & r_* \rightarrow \infty, \\ A_l^{\text{in}}(\omega) T_l(\omega) e^{-i\omega r_*} & r_* \rightarrow -\infty. \end{cases} \quad (6.19)$$

When the amplitude of the incoming wave $A_l^{\text{in}}(\omega)$ is nonzero, the physical information is contained in the reflection and transmission (*i.e.*, absorption) amplitudes, $R_l(\omega)$ and $T_l(\omega)$. We will solve this problem of scattering and absorption by the black hole, and in particular compute the absorption probability

$$\gamma_l(\omega) = |T_l(\omega)|^2. \quad (6.20)$$

The condition $A_l^{\text{in}}(\omega) = 0$ defines a different kind of problem: the determination of the spectrum of quasinormal modes of the black hole, which appear as poles in $T_l(\omega)$ and $R_l(\omega)$. This is a subtle eigenvalue problem to solve in the near region, and we postpone its detailed study to future work.

6.3 Integrating out the near region

In order to simplify the notation, we now set

$$r_0 = 1, \quad (6.21)$$

so that

$$f(r) = 1 - r^{-n}. \quad (6.22)$$

The tortoise coordinate r_* is not quite appropriate in the near region $-\infty < r_* < r_{\max}$: the non-trivial features of the potential (6.14) in this region are erased in the limit (6.18) in which r_* remains fixed as $n \rightarrow \infty$. Although we could instead keep $\hat{r}_* = nr_*$ fixed, we find more useful to work with the coordinate

$$R = r^n, \quad (6.23)$$

in terms of which the wave equation (6.7) becomes

$$\frac{d}{dR} \left(R(R-1) \frac{d}{dR} \psi \right) - \hat{l}(\hat{l}+1) \psi + \hat{\omega}^2 \frac{R^{1+2/n}}{R-1} \psi = 0. \quad (6.24)$$

To leading order at large n in the near region, where $\ln R \ll n$, this equation becomes

$$\frac{d}{dR} \left(R(R-1) \frac{d}{dR} \psi \right) - \left(\omega_c^2 - \frac{1}{4} \right) \psi + \hat{\omega}^2 \frac{R}{R-1} \psi = 0, \quad (6.25)$$

where instead of \hat{l} we use ω_c , defined in (6.17). The expansion breaks down when $\hat{\omega}$ is of order n or higher. Then our calculations apply in the range $\omega \ll n^2$.

The general solution to this equation is

$$\begin{aligned}\psi(R) = & A_1(R-1)^{-i\hat{\omega}} {}_2F_1(q_+, q_-, q_+ + q_-; 1-R) \\ & + A_2(R-1)^{i\hat{\omega}} {}_2F_1(1-q_+, 1-q_-, 2-q_+ - q_-; 1-R),\end{aligned}\quad (6.26)$$

where

$$q_{\pm} = \frac{1}{2} - i\hat{\omega} \pm \sqrt{\omega_c^2 - \hat{\omega}^2}. \quad (6.27)$$

The regularity (ingoing) boundary condition at the horizon (6.19) takes the form

$$\psi(R)\Big|_{R=1} \propto (R-1)^{-i\hat{\omega}} (1 + O(n^{-1})) \quad (6.28)$$

and therefore requires that $A_2 = 0$. We use the arbitrariness in the overall amplitude to set $A_1 = 1/\sqrt{n}$ for later convenience.

The solution can now be written as

$$\begin{aligned}\psi(R) = & \frac{\Gamma(q_+ + q_-)}{\sqrt{n}} (R-1)^{-i\hat{\omega}} \left[R^{-q_-} \frac{\Gamma(q_+ - q_-)}{\Gamma(q_+)^2} {}_2F_1(q_-, q_-, 1 - q_+ + q_-; 1/R) \right. \\ & \left. + R^{-q_+} \frac{\Gamma(q_- - q_+)}{\Gamma(q_-)^2} {}_2F_1(q_+, q_+, 1 + q_+ - q_-; 1/R) \right].\end{aligned}\quad (6.29)$$

Expanding at large R yields the solution in the overlap region $1 \ll \ln R \ll n$,

$$\psi(R) = \frac{\Gamma(q_+ + q_-)}{\sqrt{n}} R^{-\frac{1+q_++q_-}{2}} \left(\frac{\Gamma(q_+ - q_-)}{\Gamma(q_+)^2} R^{q_+} + \frac{\Gamma(q_- - q_+)}{\Gamma(q_-)^2} R^{q_-} \right) + O(R^{-1}). \quad (6.30)$$

When $q_+ = q_-$, *i.e.*, $\hat{\omega} = \omega_c$, this expansion is not valid, and instead one gets terms $R^{-1/2} \ln R$. We expect that this is due to the presence of quasinormal modes. Logarithmic terms also appear when $q_+ - q_- \in \mathbb{N}$.

The flux of the scalar at the horizon, derived from the wave equation (6.9), is

$$\begin{aligned}F_{\text{horizon}} &= \frac{i}{2} \left(\phi^* \frac{d}{dr_*} \phi - \phi \frac{d}{dr_*} \phi^* \right) \Big|_{r_* \rightarrow -\infty} \\ &= \frac{in}{2} R(R-1) \left(\psi^* \frac{d}{dR} \psi - \psi \frac{d}{dR} \psi^* \right) \Big|_{R=1}.\end{aligned}\quad (6.31)$$

For our solution (6.29) we find

$$F_{\text{horizon}} = \hat{\omega}. \quad (6.32)$$

Eq. (6.30) is an important result in this analysis: by providing a boundary condition for the fields that propagate outside the ‘sphere of influence’, it codifies the physics of the region where all the black hole dynamics is concentrated.

6.4 Far region waves

In the far region we set $f(r) \rightarrow 1 + O(e^{-n})$: the wave propagates effectively in flat space, obeying the equation

$$\frac{1}{r^{n+1}} \frac{d}{dr} \left(r^{n+1} \frac{d}{dr} \psi(r) \right) + n^2 \left(\hat{\omega}^2 - \frac{\hat{l}(\hat{l}+1)}{r^2} \right) \psi(r) = 0. \quad (6.33)$$

This is solved in terms of Bessel functions,

$$\psi(r) = C_1 \frac{J_{n\omega_c}(n\hat{\omega}r)}{r^{n/2}} + C_2 \frac{Y_{n\omega_c}(n\hat{\omega}r)}{r^{n/2}}. \quad (6.34)$$

From the behavior at large r

$$\psi(r) \simeq \frac{1}{\sqrt{2\pi\omega} r^{n+1}} \left((C_1 - iC_2) e^{i\omega r} + (C_1 + iC_2) e^{-i\omega r} \right) \quad (6.35)$$

we infer the incoming amplitude and the incoming flux from infinity,

$$F_{\text{in}} = \frac{ir^{n+1}}{2} \left(\psi_{\text{in}}^* \frac{d}{dr} \psi_{\text{in}} - \psi_{\text{in}} \frac{d}{dr} \psi_{\text{in}}^* \right) = \frac{1}{2\pi} |C_1 + iC_2|^2. \quad (6.36)$$

Quasinormal modes would be obtained under the condition $C_1 + iC_2 = 0$.

In the overlap region, and to leading order at large n , this solution gives (see appendix B.1)

$$\psi(r) \rightarrow \begin{cases} \frac{R^{-\frac{1+q_++q_-}{2}}}{\sqrt{2\pi n\omega_c \tanh \alpha_0}} \left(K_{\hat{\omega}} C_1 R^{q_+} - \frac{2C_2}{K_{\hat{\omega}}} R^{q_-} \right), & \hat{\omega} < \omega_c, \\ \frac{R^{-\frac{1+q_++q_-}{2}}}{\sqrt{2\pi n\omega_c \tan \beta_0}} \left((C_1 - iC_2) K_{\hat{\omega}} R^{q_+} + \frac{C_1 + iC_2}{K_{\hat{\omega}}} R^{q_-} \right), & \hat{\omega} > \omega_c, \end{cases} \quad (6.37)$$

with

$$K_{\hat{\omega}} = \begin{cases} e^{-n\omega_c(\alpha_0 - \tanh \alpha_0)} & \hat{\omega} < \omega_c, \\ e^{-in\omega_c(\beta_0 - \tan \beta_0) - i\pi/4} & \hat{\omega} > \omega_c, \end{cases} \quad (6.38)$$

and α_0 and β_0 defined by

$$\frac{\hat{\omega}}{\omega_c} = \begin{cases} \text{sech } \alpha_0, & \hat{\omega} < \omega_c, \\ \sec \beta_0, & \omega_c < \hat{\omega}, \end{cases} \quad (6.39)$$

so that

$$q_+ - q_- = 2\sqrt{\omega_c^2 - \hat{\omega}^2} = 2\omega_c \tanh \alpha_0 = 2i\omega_c \tan \beta_0. \quad (6.40)$$

6.5 Matching and analysis of results

Matching the coefficients in eqs. (6.30) and (6.37) we find

$$\begin{aligned} C_1 &= \frac{\sqrt{\pi(q_+ - q_-)} \Gamma(q_+ + q_-) \Gamma(q_+ - q_-)}{K_{\hat{\omega}} \Gamma(q_+)^2}, \\ C_2 &= -\frac{K_{\hat{\omega}} \sqrt{\pi(q_+ - q_-)} \Gamma(q_+ + q_-) \Gamma(q_- - q_+)}{2\Gamma(q_-)^2}, \end{aligned} \quad (6.41)$$

when $\hat{\omega} < \omega_c$, and

$$\begin{aligned} C_1 - iC_2 &= \frac{\sqrt{i\pi(q_+ - q_-)} \Gamma(q_+ + q_-) \Gamma(q_+ - q_-)}{K_{\hat{\omega}} \Gamma(q_+)^2}, \\ C_1 + iC_2 &= \frac{K_{\hat{\omega}} \sqrt{i\pi(q_+ - q_-)} \Gamma(q_+ + q_-) \Gamma(q_- - q_+)}{\Gamma(q_-)^2}. \end{aligned} \quad (6.42)$$

when $\hat{\omega} > \omega_c$.

This solves the problem of scalar field propagation in the presence of the black hole, since using these results we obtain the reflection and transmission amplitudes

$$R_l(\omega) = \frac{C_1 - iC_2}{C_1 + iC_2}, \quad T_l(\omega) = \frac{\sqrt{2\pi\hat{\omega}}}{C_1 + iC_2}, \quad (6.43)$$

which satisfy $|R_l|^2 + |T_l|^2 = 1$. A simple quantity of interest is the absorption probability,

$$\gamma_l(\omega) = \frac{F_{\text{horizon}}}{F_{\text{in}}} = \frac{2\pi\hat{\omega}}{|C_1 + iC_2|^2}. \quad (6.44)$$

Observe that all the dependence on n in C_1 and C_2 is contained in the factor $K_{\hat{\omega}}$.

6.5.1 Low frequency: $\hat{\omega} < \omega_c$

Since $\alpha_0 - \tanh \alpha_0 > 0$, in this regime $K_{\hat{\omega}}$ is exponentially small in n , except for $\omega_c - \hat{\omega} \sim n^{-2/3}$ where $K_{\hat{\omega}}$ rapidly approaches 1. We can write

$$K_{\hat{\omega} < \omega_c} = e^{n\sqrt{\omega_c^2 - \hat{\omega}^2}} \left(\frac{\omega_c + \sqrt{\omega_c^2 - \hat{\omega}^2}}{\hat{\omega}} \right)^{-n\omega_c}. \quad (6.45)$$

Given that $K_{\hat{\omega}} \ll 1$, the amplitude is dominated by $|C_1| \gg |C_2|$ and we approximate

$$\begin{aligned} \gamma_l(\omega) &\simeq \frac{2\pi\hat{\omega}}{|C_1|^2} \\ &= \frac{\hat{\omega} K_{\hat{\omega}}^2}{\sqrt{\omega_c^2 - \hat{\omega}^2} \Gamma(q_+ - q_-)^2} \frac{|\Gamma(q_+)|^4}{|\Gamma(1 + i2\hat{\omega})|^2}, \end{aligned} \quad (6.46)$$

which is strongly suppressed. More explicitly, if $\hat{\omega} \ll \omega_c$, and since $\omega_c \geq 1/2$, we can write

$$K_{\hat{\omega}}^2 \simeq \left(\frac{e\hat{\omega}}{2\omega_c} \right)^{2n\omega_c} \ll 1, \quad (6.47)$$

with all the other factors in (6.46) remaining of order one. Thus, restoring the radius r_0 and $\omega = n\hat{\omega}$ for clearer illustration, we conclude that waves of frequencies $\omega \lesssim n/r_0$ are very strongly reflected by the black hole and interact very little with it.

At very low frequencies $\omega r_0 \ll 1$ we can check against earlier results. Consider s-waves, $l = 0$, *i.e.*, $\omega_c = 1/2$, which are the dominant component of the absorption. In this case we have

$$\gamma_l(\omega) \simeq \frac{2\omega r_0}{n} K_{\hat{\omega}}^2 \quad (6.48)$$

with

$$K_{\hat{\omega}}^2 \simeq \left(\frac{e\omega r_0}{n}\right)^n \left(1 - \frac{\omega^2 r_0^2}{n} + O(\omega^3, n^{-2})\right) \quad (6.49)$$

$$\simeq \left(\frac{\omega r_0}{2}\right)^n \frac{n\pi}{\Gamma((n+2)/2)^2} \left(1 - \frac{\omega^2 r_0^2}{n} + O(\omega^3, n^{-2})\right), \quad (6.50)$$

where we have used Stirling's formula. Introducing the horizon area $A_H = r_0^{n+1} \Omega_{n+1}$ we find

$$\gamma(\omega)_{l=0} = \frac{\omega^{n+1} \Omega_{n+1}}{(2\pi)^{n+1}} A_H \left(1 - \frac{\omega^2 r_0^2}{n} + O(\omega^3, n^{-2})\right). \quad (6.51)$$

Finally projecting plane waves onto s-waves, we find the scalar absorption cross section

$$\sigma_{\text{abs}}^{\text{s-wave}} = A_H \left(1 - \frac{\omega^2 r_0^2}{n} + O(\omega^3, n^{-2})\right). \quad (6.52)$$

The leading term is the universal result of [40].

6.5.2 High frequency: $\hat{\omega} > \omega_c$

In this case $K_{\hat{\omega} > \omega_c}$ is purely imaginary, with

$$|K_{\hat{\omega} > \omega_c}| = 1. \quad (6.53)$$

When $\hat{\omega} \gg \omega_c$ it can be approximated by $K_{\hat{\omega} > \omega_c} \simeq e^{-in\hat{\omega}}$.

In contrast to the previous regime, the absorption probability now does not depend on $K_{\hat{\omega}}$. It takes the simple form

$$\gamma_l(\hat{\omega}) = \frac{\sinh(2\pi\hat{\omega}) \sinh\left(2\pi\sqrt{\hat{\omega}^2 - \omega_c^2}\right)}{\left(\cosh\left[\pi\left(\hat{\omega} + \sqrt{\hat{\omega}^2 - \omega_c^2}\right)\right]\right)^2}. \quad (6.54)$$

When $\hat{\omega} \gg \omega_c$ this becomes

$$\gamma_l(\omega) = 1 - O\left(e^{-2\pi\hat{\omega}}\right), \quad (6.55)$$

which is the expected result: the black hole is an almost perfect absorber at very high frequencies.

Note that the absence of a dependence on n in (6.54) implies a scaling behavior with ω and l of the absorption probability at large n .

6.6 Effective scalar wave dynamics

Matching constructions like we have performed admit an interpretation as effective theories. In our case, the theory consists of scalar waves that propagate in flat space. When they reach a horizon (at $r = 1$) the field modes $\psi_{\hat{\omega}l}(r)$ must satisfy the boundary condition (from (6.30)) that

$$\left. \frac{\partial_r \psi_{\hat{\omega}l}}{\psi_{\hat{\omega}l}} \right|_{r=1} = \frac{n}{2} \left((q_+ - q_-) \frac{\Gamma(q_+ - q_-) \Gamma(q_-)^2 - \Gamma(q_- - q_+) \Gamma(q_+)^2}{\Gamma(q_+ - q_-) \Gamma(q_-)^2 + \Gamma(q_- - q_+) \Gamma(q_+)^2} - 1 \right). \quad (6.56)$$

This equation *encodes all the scalar dynamics of the black hole*, to leading order at large n . Once this condition is imposed, the reflection and transmission amplitudes for field propagation take the form that we determined above.

This effective description differs in important respects from the one that results from the more familiar study of black hole absorption at very low frequency $\omega \ll 1/r_0$ [41, 42, 43]. That analysis also performs a matched asymptotic expansion between a near region $r \ll \omega^{-1}$ and a far region $r \gg r_0$. Then the effective theory is obtained after integrating out the degrees of freedom at scales $< r_0$. In the large n effective theory, instead, we integrate the physics near the horizon at scales $< r_0/D$.

This distinction is important. The conventional low-frequency effective theory treats the black hole as a point particle: waves with $\omega \ll 1/r_0$ do not resolve the size of the horizon. The conditions on the far field are then effectively imposed at $r = 0$. In our large n effective theory, instead, the horizon radius $r_0 = 1$ remains finite (even if the horizon area vanishes at $n \rightarrow \infty$), so the boundary conditions are imposed on a sphere of finite radius. This is why we are able to capture a much larger frequency range, including $\omega > n/r_0 \gg 1/r_0$, in which the black hole acts as an almost perfect absorber: excitations of these wavelengths perceive it as a finite-size object.

6.7 Final remarks

Upside. We have obtained a solution for the scattering and absorption problem that gives, in a simple analytic expression, the amplitudes over a very wide range of frequencies (and partial waves), running from the lowest part of the spectrum until very high values. As an illustration, we not only recover the well-known universal result for the low-energy absorption cross section but also we can easily extract corrections to it, eq. (6.52), which would be very hard to obtain in other approaches.

The results also confirm the conclusions of section 4: the interaction of the black hole with waves of frequencies that remain fixed as D grows is strongly suppressed by a factor of the form $\sim (\omega r_0/D)^D$ (see *e.g.*, eq. (6.47) or (6.49)), while frequencies that scale like D interact appreciably with the black hole. In fact waves with

$$\omega \gg \frac{D}{r_0} \left(\frac{1}{2} + \frac{l}{D} \right) \quad (6.57)$$

are almost perfectly absorbed.

Our analysis also provides the solution for several types of linearized gravitational perturbations of this black hole [44]: perturbations that are tensors on S^{D-2} are governed by the same equation as (6.7) at all D , and scalar gravitational perturbations also obey, to leading order at large D , the equations (6.13), (6.14) when $l = O(D^0)$. Moreover, gauge field perturbations satisfy the same equations at large D including $\hat{l} = O(D^0)$. Shear perturbations of black branes are also known to obey the equations for massless scalars.

Downside. During the matching construction we have found that it breaks down in some specific instances.

The first one occurs when $q_+ \simeq q_-$, *i.e.*, when $\hat{\omega} \simeq \omega_c$. This is also the region in which $|C_1/C_2| \simeq 1$. Since the quasinormal modes appear when $C_1 + iC_2 = 0$, we see that our present construction is not well suited for the calculation of their frequencies. Nevertheless, this analysis shows that quasinormal modes must be expected when $\hat{\omega} \sim \omega_c$. This agrees with the WKB considerations in sec. 6.2 and refs. [35, 36, 13]. Quasinormal modes are of course very important since they are responsible for resonant scattering which results in damped ringing at their frequencies. We expect that a modification of our technique will allow an analytic solution of the quasinormal modes and their frequencies.

Second, our matching is also incorrectly performed when $q_+ - q_- \in \mathbb{N}$. While the matching result for C_1 may still be correct, the matching of C_2 is more complicated.

Our solution should lose accuracy around these special frequencies. For instance, at all of them the absorption appears to vanish since C_2 diverges, but this conclusion is not reliable. In contrast, for all $\hat{\omega} > \omega_c$ there is no problem in matching C_1 and C_2 and our results in this range away from $\hat{\omega} \sim \omega_c$ are sound.

Finally, the effective theory approach fails to apply for the ultra-high frequencies and angular momenta in the range $\omega r_0, l \gtrsim D^2$. The wavelength of these excitations is so short that they are insensitive to the curvature and they do not distinguish between near and far regions. Still, our expression for the absorption probability can be expected to smoothly merge with the result at these ultra-high frequencies when $\omega r_0 \gtrsim D^2, l$, since in this case the deviations from $\gamma_l(\omega) = 1$ must be extremely small. However, the range $\omega r_0 \sim l \gg D^2$ seems to lie outside the large D techniques of this section.

Aside: near-horizon conformal symmetry? The appearance of hypergeometric functions in the near-region solution is suggestive of the presence of a two-dimensional conformal symmetry governing the amplitudes [45, 46]. Although in this article we will not pursue this idea, let us mention a potentially relevant fact that arises when $q_+ - q_- \in \mathbb{N}$,¹¹ which is always in the regime $\hat{\omega} < \omega_c$. For odd $q_+ - q_- = 2m + 1$, the absorption probability

¹¹In these cases the matching for C_2 is not valid, but we expect that the result for C_1 , which is what we use, remains valid.

is

$$\gamma^{\text{odd}}(\omega) = \frac{2\hat{\omega}K_{\hat{\omega}}^2}{\Gamma(2m+1)\Gamma(2m+2)} \frac{\left|\Gamma(1+m+i\frac{\omega}{4\pi T_H})\right|^4}{\left|\Gamma(1+i\frac{\omega}{2\pi T_H})\right|^2}, \quad (6.58)$$

and for even $q_+ - q_- = 2m$,

$$\gamma^{\text{even}}(\omega) = \frac{2\hat{\omega}K_{\hat{\omega}}^2}{\Gamma(2m)\Gamma(2m+1)} \frac{\left|\Gamma(\frac{1}{2}+m+i\frac{\omega}{4\pi T_H})\right|^4}{\left|\Gamma(1+i\frac{\omega}{2\pi T_H})\right|^2}. \quad (6.59)$$

Using

$$\begin{aligned} \left|\Gamma(1+m+ix)\right|^2 &= \frac{2\pi x e^{-\pi x}}{1-e^{-2\pi x}} \prod_{s=1}^m (s^2+x^2), \\ \left|\Gamma(\frac{1}{2}+m+ix)\right|^2 &= \frac{2\pi e^{-\pi x}}{1+e^{-2\pi x}} \prod_{s=1}^m (s^2+x^2), \end{aligned} \quad (6.60)$$

the absorption factors can be written as bosonic or fermionic Boltzmann thermal functions at temperature T_H (or two sectors at $T_H/2$).

The conformal symmetry in [46] appears in the low frequency regime $\omega r_0 \ll 1$. As discussed in sec. 6.6, our approach can deal with much larger frequencies, capturing the dynamics up to $\omega < D^2/r_0$. Then the amplitudes and absorption probabilities above, although similar to the ones in [46], differ from them. It would be very interesting if the large D effective description for the black hole took the form of a two-dimensional conformal theory.

7 Black brane instability

In the previous section we have solved a scattering problem, namely the interaction of the black hole with waves that propagate outside it. In this section we investigate a problem closer in spirit to quasinormal mode analysis, where we study the dynamics of the black hole itself. This is, we solve an eigenvalue problem for the field in the near region with boundary conditions that correspond to the absence of any external perturbing sources outside the black hole. The modes we seek differ from quasinormal ones in that they correspond to an instability.

Refs. [23, 24] proved, through a numerical solution of linearized perturbation equations, that the black branes of (2.15) are unstable to fluctuations along their worldvolume, $\delta g_{\mu\nu} \sim e^{\Omega t + i\mathbf{k}\cdot\mathbf{z}}$. Besides demonstrating the large D expansion in a different problem, the determination of the spectrum $\Omega(k)$ is an excellent benchmark for large D studies: good numerical results are available in several dimensions, but also there exist analytical approximate results [6, 7, 9, 21]. Thus we can test both the accuracy of the method when applied to finite values of D , and its effectiveness in comparison to other approaches. The outcome is very good on both counts.

7.1 Perturbation equations

At linearized order the perturbation problem depends on

$$n = D - p - 3 \quad (7.1)$$

but not on D and p separately, so in this section we will use n as the expansion parameter. To lighten the notation we set $r_0 = 1$ like in the previous section.

The Gregory-Laflamme problem involves perturbations that are scalars on S^{n+1} . There is only one physical degree of freedom, which by an appropriate choice of gauge can be chosen to be

$$\delta g_{tr} = \eta(r) e^{\Omega t + i k z}, \quad (7.2)$$

all other metric components being obtainable from this one. The linearized perturbation equation is

$$\eta'' + P(r)\eta' + Q(r)\eta = 0 \quad (7.3)$$

where the functions $P(r)$ and $Q(r)$ are [24]

$$P(r) = \frac{1}{r f A(r)} \left[3n^3 - 12n\Omega^2 r^2 + (3n^2 - 6n^3 - 8nk^2 r^2 - 4r^2\Omega^2 + 8n\Omega^2 r^2)f - (6n^2 - 3n^3 + 4k^2 r^2 - 4nk^2 r^2)f^2 + 3n^2 f^3 \right], \quad (7.4)$$

$$Q(r) = \frac{1}{r^2 f^2 A(r)} \left[(n^2 - \Omega^2 r^2)(n^2 - 4\Omega^2 r^2) + (3n^3 - n^4 + n^2 k^2 r^2 + 10n^2 \Omega^2 r^2 + 8k^2 \Omega^2 r^4)f + (n^2(1 - 6n - n^2) + 2k^2 r^2(2k^2 r^2 - 2n - n^2) + \Omega^2 r^2(4 + 4n - 5n^2))f^2 + (-2n^2 + 3n^3 + n^4 + 4k^2 r^2 + 8nk^2 r^2 + n^2 k^2 r^2)f^3 + n^2 f^4 \right], \quad (7.5)$$

with

$$A(r) = n^2 - 4\Omega^2 r^2 - (4k^2 r^2 + 2n^2)f + n^2 f^2. \quad (7.6)$$

We shall solve the boundary value problem that results from requiring asymptotic flatness at infinity and regularity at the horizon. Note that P and Q have a simple pole at $r = r_s > 1$ where $A(r_s) = 0$. This is a regular singular point of the equation. We have analyzed this point and checked that the solution that we find below is indeed regular there.

Taking cue from the result (2.18) that the zero-mode wavenumber scales like $1/\sqrt{n}$, we define

$$\hat{k} = \frac{k}{\sqrt{n}}, \quad (7.7)$$

and regard \hat{k} as being $O(n^0)$, which allows us to keep track of very short wavelengths $\sim r_0/\sqrt{n}$. In contrast we take $\Omega = O(n^0)$.

We solve the problem by matching the solutions in the near and far regions of sec. 6.1. Our method is an adaptation and extension of ref. [7].

7.2 Far region

In this region r^{-n} is a quantity that is exponentially small in $1/n$ and therefore does not yield any perturbative $1/n$ corrections. Eq. (7.3) for $\eta^{(\text{far})}$ becomes the flat space equation

$$\frac{d^2 \eta^{(\text{far})}}{dr^2} + \frac{n+1}{r} \frac{d\eta^{(\text{far})}}{dr} - \left(\frac{n+1}{r^2} + n\hat{k}^2 + \Omega^2 \right) \eta^{(\text{far})} = 0. \quad (7.8)$$

Introducing the notations $\nu = (n+2)/2$ and $k_\Omega = \sqrt{n\hat{k}^2 + \Omega^2}$, the solution that is regular at infinity is

$$\eta^{(\text{far})} \propto \frac{K_\nu(k_\Omega r)}{r^{n/2}}, \quad (7.9)$$

where $K_\nu(x)$ is the modified Bessel function of the second kind. We fix the integration constant for the amplitude of the perturbation in a manner that will simplify the matching in the overlap region. Here we use the coordinate R defined in (6.23) and expand up to next-to-next-to-leading order,

$$r = 1 + \frac{\ln R}{n} + \frac{(\ln R)^2}{2n^2} + O(n^{-3}). \quad (7.10)$$

Expanding now (7.9) for large n we find

$$\begin{aligned} \frac{K_\nu(k_\Omega r)}{r^{n/2}} = A_n & \left(\frac{1}{R} - \frac{1 + \hat{k}^2}{n} \frac{\ln R}{R} \right. \\ & \left. + \frac{1}{n^2} \frac{2(\hat{k}^4 - \Omega^2) \ln R + (1 + \hat{k}^4)(\ln R)^2}{2R} + O(n^{-3}) \right). \end{aligned} \quad (7.11)$$

Here A_n is a factor (independent of R) in which we absorb all the n -dependence from terms of the form $\propto 1/(n^i R)$ in this expansion. We choose the integration constant in $\eta^{(\text{far})}$ to eliminate this factor, so that

$$\begin{aligned} \eta^{(\text{far})} = & \frac{1}{R} - \frac{1 + \hat{k}^2}{n} \frac{\ln R}{R} \\ & + \frac{1}{n^2} \frac{2(\hat{k}^4 - \Omega^2) \ln R + (1 + \hat{k}^4)(\ln R)^2}{2R} + O(n^{-3}). \end{aligned} \quad (7.12)$$

Two comments about this result. First, note the absence of a constant term $\propto R^0$. This is a consequence of asymptotic flatness. The second independent solution to (7.8) is $I_\nu(k_\Omega r)/r^{n/2}$, which grows at $r \rightarrow \infty$: this is a non-normalizable perturbation, which amounts to introducing sources for the field at infinity. This second solution would also yield a term $\propto R^0$ in the overlap region. Therefore the requirement that in this region

$$\lim_{R \rightarrow \infty} \eta = 0, \quad (7.13)$$

is equivalent to asymptotic flatness in the far region.

Second, the expansion (7.12) involves higher powers of $\ln R$ but not of $1/R$ (this is true also if we include non-normalizable perturbations), essentially owing to the strong

localization that makes $f = 1 + O(e^{-n})$. Nevertheless, it is possible to compute the $1/R^2$ terms that come from the next-order far solution. Although we will proceed without them, they may be used to provide an alternative matching calculation. In appendix B.2 we give some details of this.

7.3 Near region

We expand in $1/n$ as

$$\eta = \sum_{j \geq 0} \frac{\eta_{(j)}(R)}{n^j}. \quad (7.14)$$

Eq. (7.3) gives an equation at each perturbative order of the form

$$\frac{d}{dR} \left(R(R-1)^3 \frac{d\eta_{(j)}}{dR} \right) + (2R-1)(R-1)\eta_{(j)} = \mathcal{S}_{(j)}, \quad (7.15)$$

where $\mathcal{S}_{(j)}$ is a j -th order source term built out of the solution up to order $j-1$. The homogeneous equation has as its independent solutions

$$u_0 = \frac{1}{R-1}, \quad v_0 = \frac{\ln(R-1) - \ln R}{R-1}. \quad (7.16)$$

With these the solution to eq. (7.15) can be found using Green's method in the form

$$\begin{aligned} \eta_{(j)} &= A_j u_0 + B_j v_0 \\ &+ u_0(R) \int_R^\infty v_0(R') \mathcal{S}_{(j)}(R') dR' + v_0(R) \int_1^R u_0(R') \mathcal{S}_{(j)}(R') dR'. \end{aligned} \quad (7.17)$$

The integration constants A_j and B_j will be determined by matching to the far region solution (7.9) at large R , and requiring regularity on the horizon at $R = 1$. This last condition can be derived by solving eq. (7.3) near $r = 1$. The regular solution is

$$\begin{aligned} \eta &\propto (r-1)^{-1+\Omega/n} (1 + O(r-1)) \\ &\propto \frac{1}{R-1} \left(1 + \frac{\Omega}{n} \ln(R-1) + \frac{\Omega^2}{2n^2} (\ln(R-1))^2 \right. \\ &\quad \left. + \frac{\Omega^3}{6n^3} (\ln(R-1))^3 + O(n^{-4}, R-1) \right). \end{aligned} \quad (7.18)$$

Matching condition. The overlap region corresponds in the near region to $R \gg 1$. Eq. (7.13) then implies that

$$\lim_{R \rightarrow \infty} \sum_j \frac{\eta_{(j)}}{n^j} = 0. \quad (7.19)$$

This condition can easily be seen to imply that the Wronskians of u_0 and $\eta_{(j)}$,

$$W[u_0, \eta_{(j)}] = R(R-1)^3 [u_0(R) \eta'_{(j)}(R) - u'_0(R) \eta_{(j)}(R)], \quad (7.20)$$

satisfy

$$\lim_{R \rightarrow \infty} \frac{1}{R^2} \sum_j \frac{W[u_0, \eta_{(j)}]}{n^j} = 0. \quad (7.21)$$

Since these Wronskians are given by

$$W[u_0, \eta_{(j)}] = \int^R dR u_0 \mathcal{S}_{(j)}, \quad (7.22)$$

then the boundary condition in the overlap region can be conveniently written in the form

$$\lim_{R \rightarrow \infty} \frac{1}{R^2} \sum_j \frac{1}{n^j} \int^R dR u_0 \mathcal{S}_{(j)} = 0. \quad (7.23)$$

Crucially, this j -th order boundary condition can be imposed with knowledge of the solution just up to $(j-1)$ -th order.

We can now proceed to solve (7.15) order by order, with the sources $\mathcal{S}_{(j)}$ computed in appendix B.3 and with the boundary conditions (7.18) and (7.23).

Zeroth order. The equation at this order is homogeneous, so

$$\eta_{(0)} = \frac{A_0}{R-1} + B_0 \frac{\ln(R-1) - \ln R}{R-1}. \quad (7.24)$$

Horizon regularity (7.18) fixes $B_0 = 0$. Matching to the far solution in the overlap region (7.12) fixes the amplitude $A_0 = 1$.

First order. The condition (7.23) for $\eta_{(1)}$ is automatically satisfied. We can integrate the source terms in (7.17) and determine the constants A_1, B_1 by imposing the boundary condition at the horizon and matching with the far region solution. Thus we obtain the first order solution in the near region as

$$\eta_{(1)} = \frac{\Omega \ln(R-1) - (1 + \hat{k}^2 + \Omega) \ln R}{R-1}. \quad (7.25)$$

Second order. The condition (7.23) to this order requires that

$$-\frac{2}{n^2}(\Omega^2 - \hat{k}^2 + 2\hat{k}^2\Omega + \hat{k}^4) = 0. \quad (7.26)$$

Choosing $\hat{k} \geq 0$, the solution to this equation that gives unstable modes is

$$\Omega = \hat{k} - \hat{k}^2. \quad (7.27)$$

This gives the dispersion relation for the Gregory-Laflamme instability to leading order at large n .

As discussed above, this result does not require the actual second-order solution: only the source term computed with $\eta_{(1)}$ has been used. However, we will need $\eta_{(2)}$ in order to find further corrections. Integrating eq. (7.15) for $j = 2$ we find

$$\begin{aligned} \eta_{(2)} = & -\frac{\pi^2\Omega^2 - 2\pi^2\hat{k}^2 + 2\pi^2\Omega\hat{k}^2 + \pi^2\hat{k}^4}{6(R-1)} \\ & + \frac{1}{2(R-1)} \left(\Omega^2(\ln(R-1))^2 + (2\Omega + 2\hat{k}^2 + 1)(\ln R)^2 \right. \\ & \quad + 2(\hat{k}^4 - \Omega^2 - \Omega(1 + \hat{k}^2 + \Omega)\ln(R-1))\ln R \\ & \quad - 4(\hat{k}^4 + \Omega^2 + 2\hat{k}^2\Omega - \hat{k}^2)(R-1) \\ & \quad \left. - 2(\Omega^2 + \hat{k}^4 + 2\hat{k}^2\Omega - 2\hat{k}^2)\text{Li}_2(1-R) \right), \end{aligned} \quad (7.28)$$

where $\text{Li}_2(z)$ is the dilogarithm function. The integration constants A_2 and B_2 have been fixed by matching to the far solution (7.12) and to the horizon solution (7.18). In more detail, near the horizon the solution becomes

$$\begin{aligned} & \eta_{(0)} + \frac{1}{n}\eta_{(1)} + \frac{1}{n^2}\eta_{(2)} \Big|_{R=1} \\ & = \left(1 + \frac{B}{n^2}\right) \left(1 + \frac{\Omega}{n}\ln(R-1) + \frac{\Omega^2}{2n^2}(\ln(R-1))^2 + O(R-1)\right), \end{aligned} \quad (7.29)$$

where

$$B = \frac{-\pi^2\Omega^2 + 2\pi^2\hat{k}^2 - 2\pi^2\hat{k}^2\Omega - \pi^2\hat{k}^4}{6}. \quad (7.30)$$

Third order. The regularity condition (7.23) for $\eta_{(3)}$ becomes

$$\begin{aligned} & -\frac{2}{n^2}(\Omega^2 - \hat{k}^2 + 2\hat{k}^2\Omega + \hat{k}^4) \\ & - \frac{2}{n^3} \left[-\Omega^2 + 2\Omega^3 + 2\hat{k}^2 - 2\hat{k}^2\Omega + 2\hat{k}^2\Omega^2 + \hat{k}^4 - 2\hat{k}^4\Omega - 2\hat{k}^6 \right. \\ & \quad \left. + (1 + \hat{k}^2)(\Omega^2 - \hat{k}^2 + 2\hat{k}^2\Omega + \hat{k}^4)\ln R \right] \\ & = O(n^{-4}), \end{aligned} \quad (7.31)$$

whose solution

$$\Omega = \hat{k} - \hat{k}^2 - \frac{\hat{k}}{2n}(1 + 2\hat{k} - 2\hat{k}^2). \quad (7.32)$$

gives the dispersion relation to next-to-leading order in $1/n$. Again, this has been obtained before calculating $\eta_{(3)}$ from (7.17).

The boundary condition at the horizon is satisfied by setting $B_3 = B\Omega$ in (7.30). The second integral in (7.17) can be performed analytically. This implies that we can compute the behavior of the third order solution $\eta_{(3)}$ in the overlap region explicitly, which is crucial in order to impose the regularity condition (see appendix B.3). The constant A_3 is determined by matching to the far region solution (7.12). Although this can be done explicitly, it turns out that A_3 does not enter in the condition (7.23) for the fourth order solution. So we can proceed to the next step without specifying A_3 .

Fourth order. With the previous solution we can compute the source $\mathcal{S}_{(4)}$. Condition (7.23) at fourth order gives

$$\Omega = \hat{k} - \hat{k}^2 - \frac{\hat{k}}{2n}(1 + 2\hat{k} - 2\hat{k}^2) + \frac{\hat{k}}{24n^2}(9 + 24\hat{k} + 12\hat{k}^2 - 8\pi^2\hat{k}^2 + 8\pi^2\hat{k}^3 - 12\hat{k}^4). \quad (7.33)$$

In order to proceed beyond this point we should do the first integral in eq. (7.17) to impose the boundary condition on $\eta_{(4)}$ at the horizon. However, we have not managed to do this analytically. Then we cannot determine B_4 , which affects the fifth order regularity condition that would give the $1/n^3$ term in $\Omega(\hat{k})$. So we stop at this order.

Eq. (7.33) is the main result of this section.

7.4 Comparisons and accuracy

Setting $\Omega = 0$ in (7.33) gives the wavenumber \hat{k} of the threshold zero-mode. Reverting to $k = \sqrt{n}\hat{k}$, we find

$$k_{\text{GL}} = \sqrt{n} \left(1 - \frac{1}{2n} + \frac{7}{8n^2} + O(n^{-3}) \right). \quad (7.34)$$

This reproduces the result in [7], which was obtained with a method essentially similar to ours, but using a different gauge. We have discussed the interpretation of the leading order result earlier in (2.18).

Analytic approximations to $\Omega(k)$ have been computed from a rather different approach. Refs. [9, 21] solved black brane perturbations in a hydrodynamic expansion at small k for arbitrary n . Ref. [9] conjectured that the relation $\Omega = \hat{k} - \hat{k}^2$ is exact when $n \rightarrow \infty$. Our results, already in (7.27), do prove it. Ref. [21] extended the calculation to include terms up to $\propto k^3$. These hydrodynamic results and our large n expansion agree where they overlap: eq. (7.33) to order (n^{-2}, \hat{k}^3) is the same as the expansion of the result of [9, 21] to the same order.¹²

Eq. (7.33), however, also contains terms $\propto \hat{k}^4, \hat{k}^5$ which are new. They should give a more accurate dispersion relation at values $\hat{k} \sim 1$, where the hydrodynamic methods become less precise. This accuracy is apparent in figure 1. While eq. (7.33) gives a rather poor approximation to the dispersion curves for $n = 1, 2$ (which is not too surprising), it gives a very good match already for $n = 3$. Overall, eq. (7.33) is a much better fit to the entire curves than the hydrodynamic approximation in [21]. E.g., for $n = 3$ the hydrodynamic curve (which is exact in n) is better only at relatively small k ($\lesssim 0.25$).

The agreement between (7.33) and the numerical data is, for large portions of the curves, quite better than the expected error $\sim 1/n^3$. The largest deviations tend to appear near the threshold mode: for $n = 3$ we find $k_{\text{GL}}^{(\text{num})}/k_{\text{GL}}^{(\text{analytic})} \approx 0.96$, which is within the $\sim 1/n^3$ margins. At $n = 4$ the match is indeed much better, $k_{\text{GL}}^{(\text{num})}/k_{\text{GL}}^{(\text{analytic})} \approx 0.99$.

¹²See appendix C for some additional comparison.

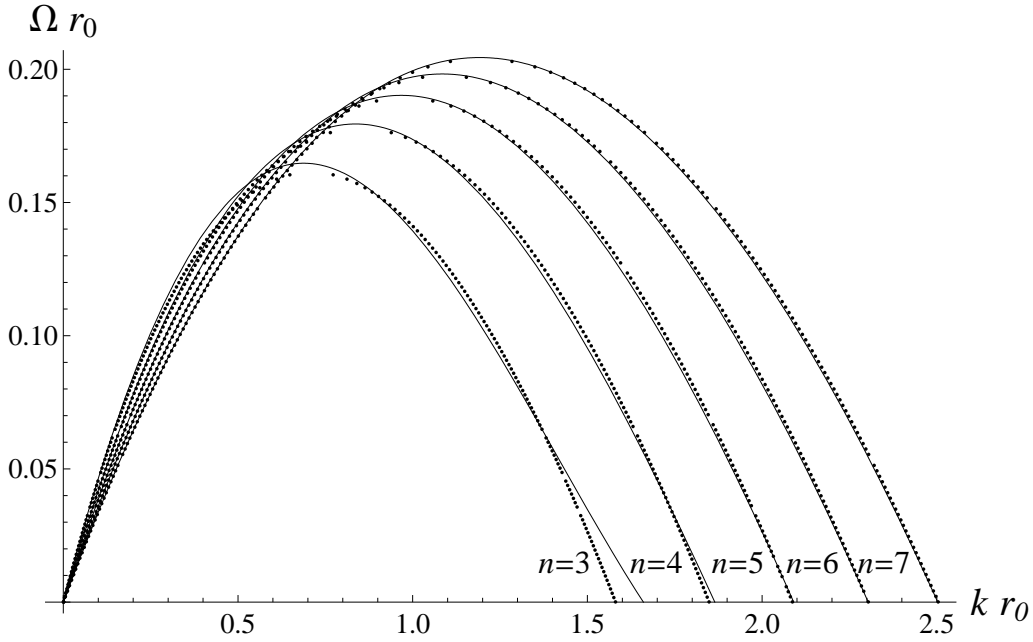


Figure 1: Dispersion relation $\Omega(k)$ of unstable modes for $n = 3, 4, 5, 6, 7$: the solid line is our analytic approximation eq. (7.33); the dots are the numerical solution (the same as in [9], courtesy of P. Figueras).

The accuracy at much larger values of n is at least as good as the precision of the numerical data we have ($\sim 10^{-5} - 10^{-6}$). This is shown in fig. 2, where we focus on the region near the zero mode where the discrepancies are possibly largest. For reference we also include the analytical result from [21].

7.5 Final remarks

AdS black branes at large D . Ref. [21] describes a map that relates the dynamics of vacuum black p -branes in $D = n + p + 3$ dimensions to the dynamics of AdS black branes in $d + 1$ dimensions, by taking $n \leftrightarrow -d$. So, by a suitable analytic continuation of n into the region of large negative numbers, we get a map of the solution in this section into a solution for perturbations of AdS_{d+1} black branes at large d . Under this map the unstable mode becomes a stable, damped, quasinormal mode.

This solution goes beyond the hydrodynamic regime by being exact in the wavenumber $\hat{k} = k/\sqrt{d}$ at each order in $1/d$. Thus, it contains information about transport coefficients at all hydrodynamic orders. In particular, since to the order $1/d^2$ that we have solved, the terms k^4 and k^5 are non-zero, this gives non-zero values for certain combinations of third and fourth order transport terms.

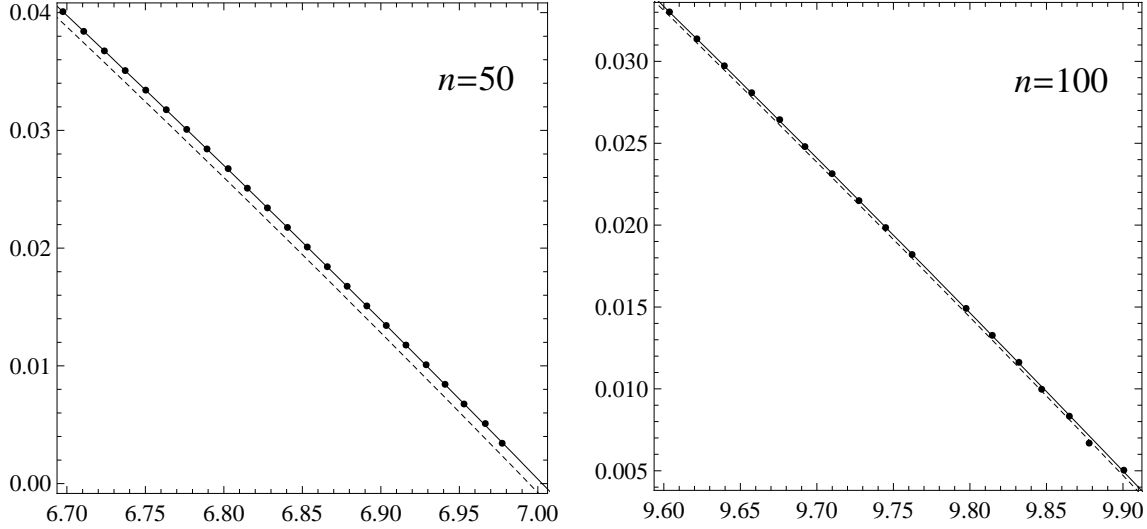


Figure 2: Dispersion relation $\Omega(k)$ for $n = 50, 100$ for k near the threshold zero-mode. The solid line is our analytic approximation eq. (7.33); the dots are the numerical solution; the dashed line is the analytic approximation of [21].

Scalings. The modes relevant in this section are localized in the sphere of influence at $r - r_0 \lesssim r_0/D$. However, the scaling of their frequencies and wavenumbers

$$\Omega \sim O(D^0), \quad k \sim O(D^{1/2}), \quad (7.35)$$

is different than the scaling $\omega \sim O(D)$ of the characteristic black hole frequencies discussed in secs. 4 and 6. They are also the scalings of a specific set of quasinormal modes of AdS black branes by the mapping above. Moreover note that $k \sim \ell_A^{-1}$, see (2.13), is a scale that has not played any role in secs. 4 and 6.

We suspect that the explanation for this scaling of black brane modes is related to the fact that they have a hydrodynamic limit. That is, these are fluctuations along a horizon that extends infinitely in one direction, while in our discussion, particularly in sec. 2.3, we made a point of taking the limit $D \rightarrow \infty$ while keeping the horizon lengths finite. This draws attention to the fact that when there are widely separate scales along the horizon (at fixed D), the dynamics at both large D and large separation of horizon scales can depend significantly on the order in which limits are taken. This issue deserves further exploration.

To conclude, the results in this section are quite encouraging for applications of the large D expansion — both because the calculations can be carried out explicitly up to a fairly high order, and because of their excellent quantitative agreement down to rather low dimensions.

8 Conclusion

Any gravitational problem that can be formulated in an arbitrary number of dimensions is susceptible to study in a large D expansion. Since some terms in the equations will drop out of the expansion, this is virtually guaranteed to yield some simplification. Problems that otherwise require numerical study may in this approach become analytically tractable.

The basic physical intuition for why and how this can be so, lies in the remarkably consistent picture we have found for General Relativity at large D . To sum it up:

- In the limit $D \rightarrow \infty$, the spacetimes are flat Minkowski geometries with ‘holes’ removed at the location of singular horizons. The radii of these holes are finite, but the area of their horizons vanishes.
- When $D \rightarrow \infty$, the holes do not interact with each other, nor with waves of any finite frequency — the horizons are reflective walls of infinitely high potential. Only for frequencies and wavenumbers that diverge with D can the interactions remain finite in the limit $D \rightarrow \infty$.
- At large but finite D the black hole has non-trivial dynamics concentrated within a thin region that extends out to a distance of order $1/D$ from the horizon.
- This dynamics can be reproduced by an effective theory of fields propagating in flat spacetime, subject to specific boundary conditions on the horizons, like (6.56) for massless scalar fields.

We have suggested an image of black holes as dust particles as capturing some features of this large D limit, in particular the absence of interactions, the vanishing cross sections, and the limiting equation of state of black branes. A different image of large- D black holes as fluid lumps was suggested in [8]. It retains the property that the radius of the black holes is finite, and that when small $1/D$ corrections are included, black strings (\sim fluid tubes) have a Plateau-like instability and break apart into black holes (\sim droplets); black holes only interact, and then can merge, when their surfaces are within very close distance of each other (like fluid drops do). It also suggests an analogy between droplet and black hole evaporation when molecular/quantum mechanical effects are included. Although we do not have an accurate and complete mapping of the large n black hole physics to either of these systems, the images still may, within their limitations, be of some intuitive help.

One may, perhaps, feel uneasy about regarding a quantity as basic as the number of dimensions as a tunable parameter of a theory. However, this is not different than in $SU(N)$ gauge theories, or actually in most theories with adjustable parameters. We are viewing the gravity theories at different values of D as being *one* uniparametric theory, and eq. (2.1) as *one* uniparametric solution of this theory.

We have studied only one of the limits of the parameter space of the theory, $D \rightarrow \infty$, but it may also be interesting to study the opposite limit. Arguably this corresponds not

to $D = 0$ or 1 but to $D = 3$. At $D = 3$, the theory (1.1) ceases to have both local dynamics and black hole solutions, but taking D as a continuous parameter one still finds non-trivial effects for $D = 3 + \epsilon$. This idea was put forward in ref. [7] to solve the problem of the Schwarzschild negative mode in an expansion in ϵ . It should be of interest to understand this expansion in more generality.¹³

Our study of gravitational radiation has been rather cursory, since at $D \rightarrow \infty$ it largely decouples from black holes — except in phenomena where the radiation probes scales extremely close to the horizon. Nevertheless, gravitational waves are a sector of the theory that deserves closer attention. Some features of classical gravitational radiation depend on the spacetime dimensionality, *e.g.*, on whether D is even or odd, as is the case for the applicability of Huygens principle [48, 39]. Further work is required to clarify the importance of all such effects in the large D expansion.

We have not considered the coupling of the gravitational field to other fields or matter systems, except for brief references to charge and the cosmological constant. The main issue when considering these additions is the choice of how the new parameters scale with D . What choice is most convenient will depend on the particular type of problem one is interested in, but often it is useful to keep fixed the length scale that characterizes the effects of the new fields on the geometry. These remarks apply as well to solutions with compactified dimensions. The size of the compact space may be fixed/grow/shrink as D increases, each choice capturing different physics. In a similar vein, in the context of higher-dimensional gravity it is natural to also include the class of Lovelock theories. Each of the new terms that these theories introduce comes with a new length parameter. Depending on how these are chosen to scale with D , different large D limits will result. The fact that the Riemann curvature tends to strongly localize close to the horizon indicates that the dust mote picture should still apply at least in some situations (*e.g.*, the ‘normal branch’ of Lovelock black holes).

Finally, another setting in which the large D expansion might be useful is the study of cosmologies of four-dimensional braneworlds in a large D bulk. Having fixed worldvolume dimension, the gravitational effect of the brane in the bulk will be strongly localized close to the brane, which may simplify some calculations.

Acknowledgments

RE acknowledges useful discussions with the authors of ref. [21], and is also grateful to the organizers and participants in the workshop “Holography, gauge theory and black holes” at the Institute of Physics, Univ. Amsterdam, in December 2012 where this work was presented. We thank Stanley Deser for correspondence on a previous version of this article. RS is grateful to the Departament de Física Fonamental at Universitat de Barcelona for hospitality during the initial stage of this project. RE was partially supported by MEC

¹³See [47] for an expansion in $D = 2 + \epsilon$.

FPA2010-20807-C02-02, AGAUR 2009-SGR-168 and CPAN CSD2007-00042 Consolider-Ingenio 2010. RS was supported by the Grant-in-Aid for the Global COE Program “The Next Generation of Physics, Spun from Universality and Emergence” from the Ministry of Education, Culture, Sports, Science and Technology (MEXT) of Japan. KT was supported by a grant for research abroad by JSPS.

A Elementary geometry at large D

Consider D -dimensional Minkowski spacetime. Using

$$\int_0^\pi d\theta (\sin \theta)^k = \sqrt{\pi} \frac{\Gamma\left(\frac{k+1}{2}\right)}{\Gamma\left(\frac{k+2}{2}\right)}, \quad (\text{A.1})$$

one obtains the area of the unit-radius sphere S^{D-2}

$$\begin{aligned} A_{\text{sph}} &= \int_0^\pi d\theta_1 \int_0^\pi d\theta_2 \dots \int_0^\pi d\theta_{D-3} \int_0^{2\pi} d\phi (\sin \theta_1)^{D-3} (\sin \theta_2)^{D-4} \dots \sin \theta_{D-3} \\ &= \Omega_{D-2} \end{aligned} \quad (\text{A.2})$$

as given in (2.3). This is not a monotonic function of D : it reaches a maximum at $D \simeq 8.257$, and then rapidly decreases as D grows. For integer D the maximum is at $D = 8$, where $\Omega_6 = 16\pi^3/15 \simeq 33$. One might be tempted to conclude that this non-monotonicity could imply qualitative differences between values of D smaller or larger than 8, and thus a potential inadequacy of the large D expansion when applied to $D < 8$.

However, this result does not make clear what we are comparing the sphere to. A more careful analysis shows that in an appropriate sense spheres do become monotonically small as D grows. The area of the circumscribed cube that contains the unit-radius sphere and is tangent to it at its faces, is

$$A_{\text{circube}} = (D-1)2^{D-1}. \quad (\text{A.3})$$

The ratio $A_{\text{sph}}/A_{\text{circube}}$ can now be seen to be a *monotonically decreasing* function of $D \geq 2$, which vanishes as

$$\frac{A_{\text{sph}}}{A_{\text{circube}}} \rightarrow \frac{\sqrt{2}}{\pi} \left(\frac{\pi e}{2D}\right)^{D/2} \rightarrow 0. \quad (\text{A.4})$$

A simple intuition for this behavior follows from considering that the length L of the diagonal of a cuboid in D spacetime dimensions is

$$L^2 = x_1^2 + \dots + x_{D-1}^2. \quad (\text{A.5})$$

Then, for a generic cuboid at large D , its diagonal length L is much larger than any of its side lengths x_i . In particular, the length L of the half-diagonal of the circumscribed cube around a unit-radius sphere is

$$L = \sqrt{D-1} \gg 1. \quad (\text{A.6})$$

Now a plain indication that the sphere is in fact semifactorially smaller than its circumscribing cube is that

$$\left(\frac{1}{L}\right)^{D-2} \rightarrow D^{-D/2}, \quad (\text{A.7})$$

which reproduces the leading behavior in (A.4).

If we consider the inscribed cube (with its vertices on the sphere) then

$$A_{\text{incube}} = (D-1)^{2-D/2} 2^{D-1}, \quad (\text{A.8})$$

which becomes much smaller than the sphere

$$\frac{A_{\text{incube}}}{A_{\text{sph}}} \rightarrow \sqrt{e} \left(\frac{\pi e}{2}\right)^{-D/2} \rightarrow 0. \quad (\text{A.9})$$

The behavior is monotonic for $D \geq 2$, but the shrinking rate is slower than in (A.4), since $A_{\text{incube}} \sim D^{-D/2}$, as follows from the above argument about the diagonals.

Similar behavior is obtained by comparing the volumes V inside these bodies, since for the unit-radius sphere and for the cube of side-length two we have

$$V = \frac{A}{D-1}. \quad (\text{A.10})$$

However, these volumes do not appear to be relevant for any purpose in this paper.

B Technical appendices to sections 6 and 7

B.1 Far scalar wave solution in the overlap region

In the overlap region we have $\ln R \ll n$ and so we can expand

$$r = 1 + \frac{1}{n} \ln R + O(n^{-2}). \quad (\text{B.1})$$

Since at large n and fixed r both the argument and the index of the Bessel functions in (6.34) are large numbers of the same order $\sim n$,¹⁴ it is appropriate to use the Debye expansion. When $\hat{\omega} < \omega_c$ it gives

$$\psi(r) = \frac{1}{\sqrt{2\pi R n \omega_c \tanh \alpha}} \left(C_1 e^{-n\omega_c(\alpha - \tanh \alpha)} - 2C_2 e^{n\omega_c(\alpha - \tanh \alpha)} + O(n^{-1}) \right), \quad (\text{B.2})$$

while at $\hat{\omega} > \omega_c$,

$$\begin{aligned} \psi(r) = \frac{1}{\sqrt{2\pi R n \omega_c \tan \beta}} & \left((C_1 - iC_2) e^{-in\omega_c(\beta - \tan \beta) - i\pi/4} \right. \\ & \left. + (C_1 + iC_2) e^{in\omega_c(\beta - \tan \beta) + i\pi/4} + O(n^{-1}) \right). \end{aligned} \quad (\text{B.3})$$

¹⁴So, again, the expansion is not valid when $\hat{\omega} \gtrsim n$.

Here α and β are defined by

$$\frac{\hat{\omega}}{\omega_c} r = \begin{cases} \text{sech } \alpha, & \hat{\omega} < \omega_c, \\ \sec \beta, & \omega_c < \hat{\omega}. \end{cases} \quad (\text{B.4})$$

Expanding in the overlap region using (B.1) we find

$$\alpha - \tanh \alpha = \alpha_0 - \tanh \alpha_0 - \tanh \alpha_0 \frac{\ln R}{n} + O(n^{-2}), \quad (\text{B.5})$$

and

$$\beta - \tan \beta = \beta_0 - \tan \beta_0 - \tan \beta_0 \frac{\ln R}{n} + O(n^{-2}). \quad (\text{B.6})$$

With this, the far solution in this region can be written as in eq. (6.37).

B.2 Black brane far solution at next order

In the far region r^{-n} is exponentially small in n and therefore it does not yield any perturbative $1/n$ corrections. In order to compute corrections to the leading far solution (7.9) we introduce an auxiliary order-counting parameter ϵ ,

$$f(r) = 1 - \epsilon r^{-n}, \quad (\text{B.7})$$

which is set to $\epsilon = 1$ at the end of the calculations. The far solution is then expanded in the form

$$\eta^{(far)} = \eta^{(0)} + \epsilon \eta^{(1)} + O(\epsilon^2). \quad (\text{B.8})$$

The first order equation in the far region is

$$\frac{d^2 \eta^{(1)}}{dr^2} + \frac{n+1}{r} \frac{d\eta^{(1)}}{dr} - \left(\frac{n+1}{r^2} + n\hat{k}^2 + \Omega^2 \right) \eta^{(1)} = - \left(P^{(1)} \frac{d\eta^{(0)}}{dr} + Q^{(1)} \eta^{(0)} \right), \quad (\text{B.9})$$

where

$$P^{(1)} = \frac{n(2n\hat{k}^2 + 3\Omega^2)}{r^{n+1}k_\Omega^2}, \quad Q^{(1)} = \frac{n^2\hat{k}^2 - (n^2\hat{k}^4 + 3n\hat{k}^2\Omega^2 + 2\Omega^4)r^2}{r^{n+2}k_\Omega^2}. \quad (\text{B.10})$$

Green's method gives the solution as

$$\eta^{(1)} = A^{(1)} \frac{K_\nu(k_\Omega r)}{r^{n/2}} + S_1 \frac{I_\nu(k_\Omega r)}{r^{n/2}} + T_1 \frac{K_\nu(k_\Omega r)}{r^{n/2}}, \quad (\text{B.11})$$

where

$$S_1 = \int_{k_\Omega r}^\infty K_\nu(x) \mathcal{S}(x) dx, \quad T_1 = \int_{k_\Omega \tilde{r}}^{k_\Omega r} I_\nu(x) \mathcal{S}(x) dx. \quad (\text{B.12})$$

\mathcal{S} is a source term defined as

$$\mathcal{S} = -k_\Omega^{-1} r^\nu \left(P^{(1)} \frac{d\eta^{(0)}}{dr} + Q^{(1)} \eta^{(0)} \right). \quad (\text{B.13})$$

We can take \tilde{r} arbitrarily since it does not affect the matching procedure.

A very lengthy calculation yields S_1 and T_1 in an unilluminating form. For the purposes of matching one only needs the expressions in the overlap region. With the normalization of the leading order solution (7.9) fixed like in sec. 7.2 (eq. (7.12)), namely

$$\eta^{(0)} = A_n^{-1} \frac{K_\nu(k_\Omega r)}{r^{n/2}}, \quad (\text{B.14})$$

then the solution in this region is

$$\begin{aligned} A_n \eta^{(1)} = & \frac{1}{R^2} + \frac{\Omega^2 - \hat{k}^2 + \hat{k}^4 - 2\hat{k}^2(1 + \hat{k}^2) \ln R}{2n\hat{k}^2 R^2} \\ & + \frac{1}{2\hat{k}^4 n^2 R^2} \left(\hat{k}^2 \Omega^2 - \Omega^4 + \hat{k}^4 + 2\hat{k}^4 \Omega^2 + 3\hat{k}^6 - \hat{k}^8 \right. \\ & \quad \left. + (\hat{k}^4 - \Omega^2 - 3\hat{k}^4 \Omega^2 + 2\hat{k}^6 + \hat{k}^8) \ln R + \hat{k}^4 (1 + \hat{k}^4) (\ln R)^2 \right) \\ & + O(n^{-3}). \end{aligned} \quad (\text{B.15})$$

The actual expression for A_n is rather complicated (dependent on n , \hat{k} and Ω) and we omit it.

This solution yields terms $\propto R^{-2}$ at orders n^0 , n^{-1} and n^{-2} . We can match them to the corresponding terms in the large R expansion of the near solutions $\eta_{(0)}$ (7.24), $\eta_{(1)}$ (7.25), and $\eta_{(2)}$ (7.28). The first of these is just a matching of the overall amplitude. The second one and the third one would provide, respectively, the dispersion relations (7.27) and (7.32).

B.3 Sources for near-region equation

The source term of the n -th order equation is given by

$$\mathcal{S}_{(n)} = \sum_{j=1}^n S_{(j)}(\eta_{(n-j)}), \quad (\text{B.16})$$

where $\eta_{(j)}$ is the j -th order solution. The $S_{(j)}$ at each order are

$$\begin{aligned} S_{(1)}(\eta) = & -2(R-1)^3 [1 + 2R(-1 + 2R)\hat{k}^2] \eta' \\ & - (R-1)^2 [3 + (1 - 4R + 8R^2)\hat{k}^2] \eta, \end{aligned} \quad (\text{B.17})$$

$$\begin{aligned} S_{(2)}(\eta) = & -8(R-1)^3 R [R\Omega^2 + (-1 + R + (-1 + 2R) \ln R)\hat{k}^2 \\ & \quad + 2R(1 - 3R + 2R^2)\hat{k}^4] \eta' \\ & - \frac{R-1}{R} [1 - 2R + R^2(1 - 5\Omega^2) - 4\Omega^2 R^3 + 8\Omega^2 R^4 \\ & \quad + 2R(R-1)(4 - 12R + 8R^2 + (1 - 4R + 8R^2) \ln R)\hat{k}^2 \\ & \quad + 8R^2(R-1)^2(1 - 2R + 4R^2)\hat{k}^4] \eta, \end{aligned} \quad (\text{B.18})$$

$$\begin{aligned}
S_{(3)}(\eta) = & -8(R-1)^3 R \left[\Omega^2 R(1+2\ln R) + \hat{k}^2(2R^2(-3+4R)\Omega^2 \right. \\
& + 2(-1+R)\ln R + (-1+2R)(\ln R)^2 \\
& + 4R(R-1)\hat{k}^2(-1+R+(-2+4R)\ln R + 2R(R-1)(-1+2R)\hat{k}^2)) \left. \right] \eta' \\
& - 2(R-1) \left[R\Omega^2(2(R-1)(-1+4R) + (-5-4R+8R^2)\ln R) \right. \\
& + (R-1)\hat{k}^2(4(1+R(-2+R+R(-1-4R+8R^2)\Omega^2)) \\
& + 8(R-1)(-1+2R)\ln R + (1-4R+8R^2)(\ln R)^2 \\
& + 16R(R-1)\hat{k}^2(1-3R+2R^2 + (1-2R+4R^2)\ln R \\
& \left. + R(R-1)(1-2R+4R^2)\hat{k}^2)) \right] \eta
\end{aligned} \tag{B.19}$$

and

$$\begin{aligned}
S_{(4)}(\eta) = & -\frac{16R(R-1)^3}{3} \left[3R\Omega^2(2R^2\Omega^2 + \ln R + (\ln R)^2) + \hat{k}^2(12\Omega^2 R^2(R-1) \right. \\
& + 12R^2(-3+4R)\Omega^2 \ln R + 3(R-1)(\ln R)^2 + (-1+2R)(\ln R)^3 \\
& + 24(R-1)R\hat{k}^2(R^2(-2+3R)\Omega^2 + (-1+R+(-1+2R)\ln R)\ln R \\
& \left. + (R-1)R\hat{k}^2(-1+R+(-3+6R)\ln R + 2(R-1)R(-1+2R)\hat{k}^2)) \right] \eta' \\
& - \frac{2(R-1)}{3} \left[3R\Omega^2(4(R-1)(-1+R+2R^2(1+2R)\Omega^2) + 4(R-1)(-1+4R)\ln R \right. \\
& + (-5-4R+8R^2)(\ln R)^2) + 2(R-1)\hat{k}^2(12(R-1)R^2(-3+8R)\Omega^2 \\
& + 12(1+R(-2+R+2R(-1-4R+8R^2)\Omega^2)\ln R \\
& + 12(R-1)(-1+2R)(\ln R)^2 + (1-4R+8R^2)(\ln R)^3 \\
& + 24(R-1)R\hat{k}^2((R-1)^2 + 6R^3(-1+2R)\Omega^2 \\
& + 2\ln R(2-6R+4R^2 + (1-2R+4R^2)\ln R) \\
& + 2(R-1)R\hat{k}^2(2-6R+4R^2 + 3(1-2R+4R^2)\ln R \\
& \left. + 2(R-1)R(1-2R+4R^2)\hat{k}^2)) \right] \eta.
\end{aligned} \tag{B.20}$$

Sources at large R. The integrations constants A_i and B_i at i -th order in (7.17) are determined by the boundary conditions at $R = 1$ and $R \gg 1$. This i -th order solution contributes to the large R condition for the $(i+1)$ -th order solution through $S_{(1)}(\eta_{(i)})$. Since $S_{(i)}(\eta)$ is linear in η , the contributions of A_i and B_i can be obtained independently. Now,

$$S_{(1)}(A_i u_0 + B_i v_0) = -A_i(1 + \hat{k}^2)R - B_i(8R^2 - 12R)\hat{k}^2 + O(R^0), \tag{B.21}$$

so the leading term at large R is controlled by B_i , not A_i . This source term is contained in the condition at large R as

$$\frac{1}{R^2} \int^R u_0(R') S_{(1)}(A_i u_0 + B_i v_0) dR' = -4\hat{k}^2 B_i + O(R^{-1}), \tag{B.22}$$

i.e., only B_i enters in the large R condition for the $(i+1)$ -th order solution. This is why in sec. 7.3 we can proceed from the third to the fourth order without A_3 .

C Hydrodynamic vs. large D expansions

When refs. [9, 21] compared the hydrodynamical and numerical calculations of $\Omega(k)$, it was observed that the agreement improves for larger n . The proposed explanation for this relies on a conjecture about the large n -dependence of higher-order hydrodynamic transport coefficients. More precisely, the large D expansion in this article is of the form

$$\Omega = \hat{k} \left(1 - \hat{k} + \frac{b_1(\hat{k})}{n} + \frac{b_2(\hat{k})}{n^2} + \dots \right), \quad (\text{C.1})$$

In the hydrodynamic expansion it seems more appropriate to keep fixed $T = n/(4\pi r_0)$, instead of r_0 . Rescaling $\tilde{\Omega} = (n+1)\Omega$, $\tilde{k} = \sqrt{n+1}k$, the expansion is

$$\tilde{\Omega} = \tilde{k} \left(1 - \frac{n+2}{n+1} \frac{\tilde{k}}{4\pi T} + c_1(n) \left(\frac{\tilde{k}}{4\pi T} \right)^2 + c_2(n) \left(\frac{\tilde{k}}{4\pi T} \right)^3 + \dots \right). \quad (\text{C.2})$$

The expansion variables in the two cases are equivalent at large n , since then $\hat{k} = \tilde{k}/(4\pi T)$. Nevertheless, these are clearly different expansions. It is apparent that the large- n accuracy of the hydrodynamic results requires that $c_j(n) \rightarrow 0$ when $n \rightarrow \infty$ for all j [9]. Hence, lacking an explicit calculation of, say, $c_2(n)$, we could not be sure within the hydrodynamic approach (*i.e.*, prior to comparing to the numerical results) that at large n there will not remain a term $\propto \hat{k}^4$ in the dispersion relation at leading order.

The $c_j(n)$ are obtained from effective hydrodynamic transport coefficients computed from black brane perturbations. While it seems possible that their leading large n scaling can be determined from generic features of higher-dimensional gravity, the required behavior has not been derived yet within the hydrodynamic approach. Our calculation of the dispersion relation in the large n expansion can be regarded as a proof of it.

The hydrodynamic expansion applies also for non-linear black brane perturbations. It should be interesting to investigate if the large D expansion can be useful in that problem too.

References

- [1] For a comprehensive treatment see *Black Holes in Higher Dimensions*, edited by G. T. Horowitz, Cambridge Univ. Press (2012).
- [2] A. Strominger, “The Inverse Dimensional Expansion In Quantum Gravity,” *Phys. Rev. D* **24** (1981) 3082.
- [3] N. E. J. Bjerrum-Bohr, “Quantum gravity at a large number of dimensions,” *Nucl. Phys. B* **684** (2004) 209 [hep-th/0310263].
- [4] H. W. Hamber and R. M. Williams, “Quantum gravity in large dimensions,” *Phys. Rev. D* **73** (2006) 044031 [hep-th/0512003].

- [5] F. Canfora, A. Giacomini and A. R. Zerwekh, “Kaluza-Klein theory in the limit of large number of extra dimensions,” *Phys. Rev. D* **80** (2009) 084039 [arXiv:0908.2077 [gr-qc]].
- [6] B. Kol and E. Sorkin, “On black-brane instability in an arbitrary dimension,” *Class. Quant. Grav.* **21** (2004) 4793 [gr-qc/0407058].
- [7] V. Asnin, D. Gorbonos, S. Hadar, B. Kol, M. Levi and U. Miyamoto, “High and Low Dimensions in The Black Hole Negative Mode,” *Class. Quant. Grav.* **24** (2007) 5527 [arXiv:0706.1555 [hep-th]].
- [8] M. M. Caldarelli, O. J. C. Dias, R. Emparan and D. Klemm, “Black Holes as Lumps of Fluid,” *JHEP* **0904** (2009) 024 [arXiv:0811.2381 [hep-th]].
- [9] J. Camps, R. Emparan and N. Haddad, “Black Brane Viscosity and the Gregory-Laflamme Instability,” *JHEP* **1005** (2010) 042 [arXiv:1003.3636 [hep-th]].
- [10] J. Soda, “Hierarchical dimensional reduction and gluing geometries,” *Prog. Theor. Phys.* **89** (1993) 1303.
- [11] D. Grumiller, W. Kummer and D. V. Vassilevich, “Dilaton gravity in two-dimensions,” *Phys. Rept.* **369** (2002) 327 [hep-th/0204253].
- [12] H. Yoshino and Y. Nambu, “High-energy head-on collisions of particles and hoop conjecture,” *Phys. Rev. D* **66** (2002) 065004 [gr-qc/0204060].
- [13] E. Berti, V. Cardoso and A. O. Starinets, “Quasinormal modes of black holes and black branes,” *Class. Quant. Grav.* **26** (2009) 163001 [arXiv:0905.2975 [gr-qc]].
- [14] S. Hod, “Quantum buoyancy, generalized second law, and higher-dimensional entropy bounds,” *JHEP* **1012** (2010) 033 [arXiv:1101.3151 [gr-qc]].
- [15] S. Hod, “Higher-dimensional violations of the holographic entropy bound,” *Phys. Lett. B* **695** (2011) 294 [arXiv:1106.3817 [gr-qc]].
- [16] S. Hod, “Bulk emission by higher-dimensional black holes: Almost perfect blackbody radiation,” *Class. Quant. Grav.* **28** (2011) 105016 [arXiv:1107.0797 [gr-qc]].
- [17] S. Hod, “Hyperentropic systems and the generalized second law of thermodynamics,” *Phys. Lett. B* **700** (2011) 75 [arXiv:1108.0744 [gr-qc]].
- [18] F. S. Coelho, C. Herdeiro and M. O. P. Sampaio, “Radiation from a D-dimensional collision of shock waves: a remarkably simple fit formula,” *Phys. Rev. Lett.* **108** (2012) 181102 [arXiv:1203.5355 [hep-th]].

- [19] F. S. Coelho, C. Herdeiro, C. Rebelo and M. Sampaio, “Radiation from a D-dimensional collision of shock waves: higher order set up and perturbation theory validity,” arXiv:1206.5839 [hep-th].
- [20] F. S. Coelho, C. Herdeiro, C. Rebelo and M. O. P. Sampaio, “Radiation from a D-dimensional collision of shock waves: an insight allowed by the D parameter,” arXiv:1301.1073 [gr-qc].
- [21] M. M. Caldarelli, J. Camps, B. Gouteraux and K. Skenderis, “AdS/Ricci-flat correspondence and the Gregory-Laflamme instability,” arXiv:1211.2815 [hep-th].
- [22] F. R. Tangherlini, “Schwarzschild field in n dimensions and the dimensionality of space problem,” *Nuovo Cim.* **27** (1963) 636.
- [23] R. Gregory and R. Laflamme, “Black strings and p-branes are unstable,” *Phys. Rev. Lett.* **70** (1993) 2837 [hep-th/9301052].
- [24] R. Gregory and R. Laflamme, “The Instability of charged black strings and p-branes,” *Nucl. Phys. B* **428** (1994) 399 [hep-th/9404071].
- [25] L. Lehner and F. Pretorius, “Black Strings, Low Viscosity Fluids, and Violation of Cosmic Censorship,” *Phys. Rev. Lett.* **105** (2010) 101102 [arXiv:1006.5960 [hep-th]].
- [26] R. C. Myers and M. J. Perry, “Black Holes in Higher Dimensional Space-Times,” *Annals Phys.* **172** (1986) 304.
- [27] R. Emparan and R. C. Myers, “Instability of ultra-spinning black holes,” *JHEP* **0309** (2003) 025 [hep-th/0308056].
- [28] R. Emparan, T. Harmark, V. Niarchos and N. A. Obers, “Essentials of Blackfold Dynamics,” *JHEP* **1003** (2010) 063 [arXiv:0910.1601 [hep-th]].
- [29] R. Emparan, T. Harmark, V. Niarchos and N. A. Obers, “New Horizons for Black Holes and Branes,” *JHEP* **1004** (2010) 046 [arXiv:0912.2352 [hep-th]].
- [30] R. Emparan, “Rotating circular strings, and infinite nonuniqueness of black rings,” *JHEP* **0403** (2004) 064 [hep-th/0402149].
- [31] M. M. Caldarelli, R. Emparan and B. Van Pol, “Higher-dimensional Rotating Charged Black Holes,” *JHEP* **1104** (2011) 013 [arXiv:1012.4517 [hep-th]].
- [32] R. Emparan, T. Harmark, V. Niarchos and N. A. Obers, “Blackfolds in Supergravity and String Theory,” *JHEP* **1108** (2011) 154 [arXiv:1106.4428 [hep-th]].
- [33] E. Witten, “Anti-de Sitter space, thermal phase transition, and confinement in gauge theories,” *Adv. Theor. Math. Phys.* **2** (1998) 505 [hep-th/9803131].

- [34] R. Emparan, G. T. Horowitz and R. C. Myers, “Black holes radiate mainly on the brane,” *Phys. Rev. Lett.* **85** (2000) 499 [hep-th/0003118].
- [35] R. A. Konoplya, “Quasinormal behavior of the d-dimensional Schwarzschild black hole and higher order WKB approach,” *Phys. Rev. D* **68** (2003) 024018 [gr-qc/0303052].
- [36] E. Berti, M. Cavaglia and L. Gualtieri, “Gravitational energy loss in high-energy particle collisions: Ultrarelativistic plunge into a multidimensional black hole,” *Phys. Rev. D* **69**, 124011 (2004) [hep-th/0309203].
- [37] S. W. Hawking, “Gravitational radiation from colliding black holes,” *Phys. Rev. Lett.* **26** (1971) 1344.
- [38] D. M. Eardley and S. B. Giddings, “Classical black hole production in high-energy collisions,” *Phys. Rev. D* **66** (2002) 044011 [gr-qc/0201034].
- [39] V. Cardoso, O. J. C. Dias and J. P. S. Lemos, “Gravitational radiation in D-dimensional space-times,” *Phys. Rev. D* **67** (2003) 064026 [hep-th/0212168].
- [40] S. R. Das, G. W. Gibbons and S. D. Mathur, “Universality of low-energy absorption cross-sections for black holes,” *Phys. Rev. Lett.* **78**, 417 (1997) [hep-th/9609052].
- [41] A. A. Starobinsky and S. M. Churilov, “Amplification of electromagnetic and gravitational waves scattered by a rotating black hole”, *Zh. Eksp. Teor. Fiz.* **65** (1973) 3.
- [42] W. G. Unruh, “Absorption Cross-Section of Small Black Holes,” *Phys. Rev. D* **14** (1976) 3251.
- [43] T. Harmark, J. Natario and R. Schiappa, “Greybody Factors for d-Dimensional Black Holes,” *Adv. Theor. Math. Phys.* **14**, 727 (2010) [arXiv:0708.0017 [hep-th]].
- [44] H. Kodama and A. Ishibashi, “A Master equation for gravitational perturbations of maximally symmetric black holes in higher dimensions,” *Prog. Theor. Phys.* **110** (2003) 701 [hep-th/0305147].
- [45] J. M. Maldacena and A. Strominger, “Black hole grey body factors and d-brane spectroscopy,” *Phys. Rev. D* **55**, 861 (1997) [hep-th/9609026].
- [46] A. Castro, A. Maloney and A. Strominger, “Hidden Conformal Symmetry of the Kerr Black Hole,” *Phys. Rev. D* **82**, 024008 (2010) [arXiv:1004.0996 [hep-th]].
- [47] D. Grumiller and R. Jackiw, “Liouville gravity from Einstein gravity,” arXiv:0712.3775 [gr-qc].
- [48] H. Ooguri, “Spectrum Of Hawking Radiation And Huygens’ Principle,” *Phys. Rev. D* **33** (1986) 3573.